

**UNIVERSITY OF OKLAHOMA
GRADUATE COLLEGE**

**THERMALLY PERFECT, CALORICALLY IMPERFECT
TAYLOR-MACCOLL FLOW**

**A THESIS
SUBMITTED TO THE GRADUATE FACULTY
in partial fulfillment of the requirements for the
MASTER OF SCIENCE**

**By
DIETRICH RUDOLF LAMPE
Norman, Oklahoma
1994**

**THERMALLY PERFECT, CALORICALLY IMPERFECT
TAYLOR-MACCOLL FLOW**

A THESIS

**APPROVED FOR THE SCHOOL OF AEROSPACE AND
MECHANICAL ENGINEERING**

By

G. Emanuel

[Signature]

Prof. Eugene C. Tsieng

c Copyright by Dietrich Rudolf Lampe 1994
All rights reserved

ACKNOWLEDGEMENTS

I would like to thank my thesis committee chairman, Prof. George Emanuel. He has been very patient and supportive in my efforts to obtain a masters degree. His outstanding experience and academic excellence helped me overcome the problems.

My thanks go also to the other members of my thesis committee, Prof. Lai and Prof. Striz. I am grateful to you for taking time to critique my work, and to be part of this committee.

Another great contributor to my success was the Fulbright-Commission, the Commission for Educational Exchange between the United States of America and the Federal Republic of Germany.

Finally, my heartfelt thanks goes out to my family, especially my parents, for their unlimited and continued support throughout the years.

TABLE OF CONTENTS

	Page
ACKNOWLEDGEMENTS	iv
LIST OF TABLES	vi
LIST OF FIGURES	vii
NOMENCLATURE	ix
ABSTRACT	xi
Chapters	
1. INTRODUCTION	1
2. GAS MODELS	3
3. HOMENTROPIC AND HOMENERGETIC EQUATIONS	7
4. TAYLOR-MACCOLL FLOW	10
4.1 SHOCK DYNAMICS	11
4.2 FLOW FIELD BETWEEN SHOCK AND BODY	17
4.2.1 PERFECT GAS	25
4.2.2 IMPERFECT GAS	27
4.3 SURFACE PRESSURE COEFFICIENT	30
5. COMPUTER PROCEDURE	31
5.1 VALIDATION	41
6. RESULTS	42
6.1 $\theta_b - \beta$ PLOTS	42
6.2 $\theta_b - C_{pb}$ PLOT	43
6.3 WEAK SOLUTION COMPARISONS	48
6.4 STRONG SOLUTION COMPARISONS	52
REFERENCES	55
TABLES	57

LIST OF TABLES

Table	Page
1. β vs. θ_b for plane oblique shock; $M_1=1.2$; weak solution	57
2. β vs. θ_b for plane oblique shock; $M_1=1.2$; strong solution	58
3. β vs. θ_b for plane oblique shock; $M_1=1.5$; weak solution	59
4. β vs. θ_b for plane oblique shock; $M_1=1.5$; strong solution	60
5. β vs. θ_b for plane oblique shock; $M_1=2.0$; weak solution	61
6. β vs. θ_b for plane oblique shock; $M_1=2.0$; strong solution	62
7. β vs. θ_b for plane oblique shock; $M_1=3.0$; weak solution	63
8. β vs. θ_b for plane oblique shock; $M_1=3.0$; strong solution	64
9. β vs. θ_b for plane oblique shock; $M_1=10.0$; weak solution	65
10. β vs. θ_b for plane oblique shock; $M_1=10.0$; strong solution	66
11. β vs. θ_b for Taylor-Maccoll flow; $M_1=1.2$; weak solution	67
12. β vs. θ_b for Taylor-Maccoll flow; $M_1=1.2$; strong solution	68
13. β vs. θ_b for Taylor-Maccoll flow; $M_1=1.5$; weak solution	69
14. β vs. θ_b for Taylor-Maccoll flow; $M_1=1.5$; strong solution	70
15. β vs. θ_b for Taylor-Maccoll flow; $M_1=2.0$; weak solution	71
16. β vs. θ_b for Taylor-Maccoll flow; $M_1=2.0$; strong solution	72
17. β vs. θ_b for Taylor-Maccoll flow; $M_1=3.0$; weak solution	73
18. β vs. θ_b for Taylor-Maccoll flow; $M_1=3.0$; strong solution	74
19. β vs. θ_b for Taylor-Maccoll flow; $M_1=10.0$; weak solution	75
20. β vs. θ_b for Taylor-Maccoll flow; $M_1=10.0$; strong solution	76
21. C_{pb} vs. θ_b for Taylor-Maccoll flow; $M_1=1.2$; weak solution	77
22. C_{pb} vs. θ_b for Taylor-Maccoll flow; $M_1=1.2$; strong solution	78
23. C_{pb} vs. θ_b for Taylor-Maccoll flow; $M_1=1.5$; weak solution	79
24. C_{pb} vs. θ_b for Taylor-Maccoll flow; $M_1=1.5$; strong solution	80
25. C_{pb} vs. θ_b for Taylor-Maccoll flow; $M_1=2.0$; weak solution	81
26. C_{pb} vs. θ_b for Taylor-Maccoll flow; $M_1=2.0$; strong solution	82
27. C_{pb} vs. θ_b for Taylor-Maccoll flow; $M_1=3.0$; weak solution	83
28. C_{pb} vs. θ_b for Taylor-Maccoll flow; $M_1=3.0$; strong solution	84
29. C_{pb} vs. θ_b for Taylor-Maccoll flow; $M_1=10.0$; weak solution	85
30. C_{pb} vs. θ_b for Taylor-Maccoll flow; $M_1=10.0$; strong solution	86

Table	Page
31. β -ratio vs. M_1 for Taylor-Maccoll flow; $\theta_b=10^\circ$; weak solution	87
32. β -ratio vs. M_1 for Taylor-Maccoll flow; $\theta_b=10^\circ$; strong solution	88
33. C_{pb} -ratio vs. M_1 for Taylor-Maccoll flow; $\theta_b=10^\circ$; weak solution	89
34. C_{pb} -ratio vs. M_1 for Taylor-Maccoll flow; $\theta_b=10^\circ$; strong solution	90
35. M_2 -ratio vs. M_1 for Taylor-Maccoll flow; $\theta_b=10^\circ$; weak solution	91
36. M_2 -ratio vs. M_1 for Taylor-Maccoll flow; $\theta_b=10^\circ$; strong solution	92
37. M_b -ratio vs. M_1 for Taylor-Maccoll flow; $\theta_b=10^\circ$; weak solution	93
38. M_b -ratio vs. M_1 for Taylor-Maccoll flow; $\theta_b=10^\circ$; strong solution	94

LIST OF FIGURES

Figure	Page
1. Nomenclature for Taylor-Maccoll flow	10
2. Nomenclature for shock	11
3. θ_b vs. β for plane oblique shock	45
4. θ_b vs. β for Taylor-Maccoll flow	46
5. θ_b vs. C_{pb} for Taylor-Maccoll flow	47
6. β -comparison; $\theta_b=10^\circ$; weak solution	49
7. C_{pb} -comparison; $\theta_b=10^\circ$; weak solution	50
8. M_2 -comparison; $\theta_b=10^\circ$; weak solution	50
9. M_b -comparison; $\theta_b=10^\circ$; weak solution	51
10. β -comparison; $\theta_b=10^\circ$; strong solution	52
11. C_{pb} -comparison; $\theta_b=10^\circ$; strong solution	53
12. M_2 -comparison; $\theta_b=10^\circ$; strong solution	53
13. M_b -comparison; $\theta_b=10^\circ$; strong solution	54

NOMENCLATURE

Primary Symbols

A	Projected frontal area of the cone
a	Speed of sound
C_p	Pressure coefficient
c_p	Specific heat at constant pressure
c_v	Specific heat at constant volume
e	Internal energy
F	Force
h	Enthalpy
M	Mach number
P	Nondimensional pressure
p	Pressure
Q	Nondimensional velocity
r	Radial coordinate
R_g	Gas constant ($R_g = 8.3143 \frac{\text{kJ}}{\text{kmol K}}$)
R	Nondimensional density
s	Entropy
T	Temperature
T_v	Characteristic vibrational temperature
t	Time
u	Velocity component parallel to the centerline
V	Flow speed
v	Velocity component perpendicular to the centerline
ν	Natural frequency
x	Axial coordinate
β	Shock angle
γ	Ratio of specific heats
δ	Vibrational contribution, 0 or 1
ϕ	Streamline angle

η	Angular coordinate
ξ	Coordinate
ω	Scalar vorticity
θ	Angle (measured from center line)
Θ_v	Nondimensional temperature
ρ	Density
μ	Mach angle

Subscripts

0	Stagnation state
1	Upstream of shock
2	Downstream of shock
b	At the body
e	Electronic
min	Minimum
n	Normal component
r	Reference state
rot	Rotational
t	Tangential component
tr	Translational
vib	Vibrational

ABSTRACT

An imperfect gas model is applied to supersonic flow over a cone at zero incidence, known as Taylor-Maccoll flow. The model considers vibrational equilibrium of a diatomic gas. In air, these effects are of significance at high temperatures, e.g., above 800 K. The harmonic oscillator model of quantum mechanics is utilized to evaluate the change in molecular vibrational internal energy with temperature.

An inviscid flow with a constant stagnation enthalpy is assumed. In the region behind the shock, the flow is considered to be homentropic. The governing equations have been developed and simplified for computer use. A similarity solution is considered and the differential equations are integrated from the shock to the body.

Specified parameters are the characteristic vibrational temperature, upstream Mach number, and cone semi-vertex angle. Imperfect to perfect gas ratios are calculated for the shock angle, the Mach number behind the shock, the surface pressure coefficient, and the Mach number at the body. Properties are discussed for both the weak and strong solutions.

1. INTRODUCTION

This thesis analyzes the flow field surrounding a cone at zero incidence using an imperfect gas model. When the bow shock is attached to the vertex of the cone, this is called Taylor-Maccoll flow. In the past, this flow was discussed using only a perfect gas model and results were limited to the weak solution. In our approach, we employ a thermally perfect, but calorically imperfect, gas model.

The imperfect gas model utilizes the harmonic oscillator approximation for the vibrational energy of a diatomic species. Thus, the gas is thermally perfect but calorically imperfect. Three nondimensional parameters determine the conical flow field. These are the upstream Mach number M_1 , the semi-vertex angle θ_b of the cone, and a stagnation temperature T_0 , defined as $\Theta_{v_0} = \frac{T_v}{2T_0}$, where T_v is the characteristic vibrational temperature of the diatomic species. Results are given for $\Theta_{v_0}=0.5, 1.5,$ and 5.0 , which roughly correspond to T_0 values of 3000 K, 1000 K, and 300 K for air. As we shall see, the results with $\Theta_{v_0}=5.0$ are essentially identical to the usual calorically perfect air model, where the ratio of specific heats γ is 1.4. The formulation and results, however, are nondimensional and do not require the above T_0 values.

Results are obtained for four parameters. These are the Mach numbers just downstream of the shock and on the body, the shock wave angle, and the pressure coefficient on the body. Results are given

in graphical and tabular form and comparisons with a $\gamma=1.4$ perfect gas are provided.

This thesis is the fourth in a series of studies that applies this simplest of all imperfect gas models to basic gas dynamic flows. The first, by Christy,¹ examines isentropic flow. The second by Bultman,² deals with the normal and oblique planar shock wave. The third, by Ismail,³ treats Prandtl-Meyer flow. This thesis uses for Taylor-Maccoll flow the same nomenclature, approach, and assumptions employed in these earlier studies.

2. GAS MODELS

A gas is considered to be thermally perfect as long as it follows the equation of state

$$\frac{P}{\rho} = R_g T \quad (2-1)$$

The distinction between a calorically perfect and a calorically imperfect gas is made by the specific heat at constant volume c_v , which is given by

$$c_v = \left(\frac{\partial e}{\partial T} \right)_v \quad (2-2)$$

A calorically perfect gas has a constant c_v , while c_v is not a constant for a calorically imperfect gas. The molecules of the calorically perfect diatomic gas are regarded as rigid 'dumbbells'. In contrast to the perfect gas case, the atoms of the calorically imperfect diatomic gas oscillate about the molecules' center of mass. In order to have a suitable notation, we introduce the parameter

$$\delta = \begin{cases} 0 \Rightarrow \begin{cases} \text{vibrational effects not included, i.e.,} \\ \text{calorically perfect diatomic gas} \end{cases} \\ 1 \Rightarrow \begin{cases} \text{vibrational effects included, i.e.,} \\ \text{calorically imperfect diatomic gas} \end{cases} \end{cases}$$

The specific internal energy of the gas can be written as

$$e = e_{tr} + e_{rot} + e_{vib} + e_{el} \quad (2-3)$$

where for diatomic species

$$\begin{aligned} e_{tr} &= \text{translational contribution} = \frac{3}{2} R_g T \\ e_{rot} &= \text{rotational contribution} = R_g T \\ e_{el} &= \text{electronic contribution} = 0 \end{aligned} \quad (2-4)$$

The harmonic oscillator model of quantum mechanics provides⁴

$$e_{vib} = \text{vibrational contribution} = \frac{R_g T_v}{e^{\frac{T_v}{T}} - 1} \quad (2-5)$$

Some characteristic vibrational temperatures are⁴

$$N_2 \rightarrow 3350 \text{ K} \quad O_2 \rightarrow 2240 \text{ K} \quad CO \rightarrow 3080 \text{ K}$$

For a mixture of the diatomic molecules such as air, reference 4 suggests $T_{vair} = 3056 \text{ K}$. From equation (2-5), we have the limiting cases

$T \gg T_v$	$T \ll T_v$
$e_{vib} \Rightarrow R_g T$	$e_{vib} \Rightarrow 0$

This justifies the neglect of vibrational excitation at low temperatures and underlines the need to consider it at high temperatures.

We obtain from equations (2-4) and (2-5)

$$e = \frac{5}{2} R_g T + \delta \frac{R_g T_v}{e^{\frac{T_v}{T}} - 1} \quad (2-6)$$

Hence, we can find for the specific heat at constant volume

$$c_v = \frac{\partial e}{\partial T} = R_g \left(\frac{5}{2} + \delta \left\{ \frac{T_v/2T}{\sinh(T_v/2T)} \right\}^2 \right)$$

We introduce the nondimensional temperature

$$\Theta_v = \frac{T_v}{2T} \quad (2-7)$$

which yields

$$c_v = R_g \left(\frac{5}{2} + \delta \left\{ \frac{\Theta_v}{\sinh \Theta_v} \right\}^2 \right) \quad (2-8)$$

Since the gas is thermally perfect, we have for the specific heat at constant pressure⁴

$$c_p = c_v + R_g \quad (2-9)$$

With equations (2-8) and (2-9), it follows that

$$c_p = R_g \left(\frac{7}{2} + \delta \left\{ \frac{\Theta_v}{\sinh \Theta_v} \right\}^2 \right) \quad (2-10)$$

and the ratio of specific heats γ is given by

$$\gamma = \frac{c_p}{c_v} = \frac{7 + 2\delta \left(\frac{\Theta_v}{\sinh \Theta_v} \right)^2}{5 + 2\delta \left(\frac{\Theta_v}{\sinh \Theta_v} \right)^2} \quad (2-11)$$

As the reader can see, equation (2-11) yields the well known result, $\gamma = 1.4$, for a perfect gas.

The following equations are valid for both gas models and may be obtained by standard thermodynamic procedures⁵

$$a^2 = \gamma R_g T \quad (2-12)$$

$$e(T) = e_r + \int_{T_r}^T c_v(T') dT' \quad (2-13)$$

$$h(T) = e(T) + R_g T \quad (2-14)$$

$$s(T, \rho) = s_r + R_g \ln \frac{\rho_r}{\rho} + \int_{T_r}^T c_v(T') \frac{dT'}{T'} \quad (2-15)$$

The integrals in equation (2-13) and (2-15) can be determined using equation (2-8) and are provided by reference 5 as

$$\int_{T_r}^T c_v dT' = \frac{5}{2} R_g T_r \left(\frac{\Theta_{vr}}{\Theta_v} - 1 \right) + \delta R_g T_r \Theta_{vr} (\coth \Theta_v - \coth \Theta_{vr})$$

$$\int_{T_r}^T c_v \frac{dT'}{T'} = \frac{5}{2} R_g \ln \frac{\Theta_{vr}}{\Theta_v} + \delta R_g \left(\Theta_v \coth \Theta_v - \Theta_{vr} \coth \Theta_{vr} + \ln \frac{\sinh \Theta_{vr}}{\sinh \Theta_v} \right)$$

Hence, the internal energy and the specific entropy become

$$e(T) = e_r + \frac{5}{2} R_g T_r \left(\frac{\Theta_{vr}}{\Theta_v} - 1 \right) + \delta R_g T_r \Theta_{vr} (\coth \Theta_v - \coth \Theta_{vr}) \quad (2-16)$$

$$s = s_r + R_g \ln \frac{\rho_r}{\rho} + \frac{5}{2} R_g \ln \frac{\Theta_{vr}}{\Theta_v} + \delta R_g \left(\Theta_v \coth \Theta_v - \Theta_{vr} \coth \Theta_{vr} + \ln \frac{\sinh \Theta_{vr}}{\sinh \Theta_v} \right) \quad (2-17)$$

3. HOMENTROPIC AND HOMENERGETIC EQUATIONS

In this chapter, equations are derived for the homentropic and constant stagnation enthalpy conditions. These conditions result from the assumption of an adiabatic and inviscid flow. Homentropic flow in the region behind the shock means

$$s = s_r \quad (3-1)$$

Furthermore, it is convenient to take the reference entropy as the stagnation entropy

$$s_r = s_0 \quad (3-2)$$

Putting (3-1) and (3-2) into (2-17) yields

$$-R_g \ln \frac{\rho_0}{\rho} = \frac{5}{2} R_g \ln \frac{\Theta_{v0}}{\Theta_v} + \delta R_g \left(\Theta_v \coth \Theta_v - \Theta_{v0} \coth \Theta_{v0} + \ln \frac{\sinh \Theta_{v0}}{\sinh \Theta_v} \right)$$

Combining the logarithm terms results in

$$\ln \left[\frac{\rho_0}{\rho} \left(\frac{\Theta_{v0}}{\Theta_v} \right)^{\frac{5}{2}} \left(\frac{\sinh \Theta_{v0}}{\sinh \Theta_v} \right)^{\delta} \right] = \delta (\Theta_{v0} \coth \Theta_{v0} - \Theta_v \coth \Theta_v)$$

which can be rearranged to

$$\frac{\rho}{\rho_0} = \left(\frac{\Theta_{v0}}{\Theta_v} \right)^{\frac{5}{2}} \left(\frac{\sinh \Theta_{v0}}{\sinh \Theta_v} \right)^{\delta} \exp[\delta (\Theta_v \coth \Theta_v - \Theta_{v0} \coth \Theta_{v0})] \quad (3-3)$$

It is the goal of the next derivation to provide the connection between Mach number and temperature. Stagnation enthalpy and Mach number are defined as

$$h_0 = h + \frac{1}{2}V^2 \quad (3-4)$$

$$M = \frac{V}{a} \quad (3-5)$$

Equation (2-7) may be rearranged to

$$T = \frac{T_v}{2\Theta_v} \quad (3-6)$$

After substituting equations (3-5) and (3-6) into equation (2-12), we have

$$V = M \sqrt{\frac{\gamma R_g T_v}{2\Theta_v}} \quad (3-7)$$

Introduce equations (2-14), (3-6), and (3-7) into (3-4) to yield

$$h_0 = e(T) + R_g \frac{T_v}{2\Theta_v} + \frac{R_g T_v}{4\Theta_v} \gamma M^2 \quad (3-8)$$

The internal energy e may be replaced with equation (2-16). Then we apply equation (3-6), and take the stagnation state as the reference state

$$h_0 = e_0 + \frac{5}{2} R_g \frac{T_v}{2\Theta_{v0}} \left(\frac{\Theta_{v0}}{\Theta_v} - 1 \right) + \delta R_g \frac{T_v}{2} (\coth \Theta_v - \coth \Theta_{v0}) + R_g \frac{T_v}{2\Theta_v} + \frac{R_g T_v}{4\Theta_v} \gamma M^2 \quad (3-9)$$

Write equation (2-14) for the stagnation state, and use equation (3-6) to obtain

$$h_0 = e_0 + R_g \frac{T_v}{2\Theta_{v0}} \quad (3-10)$$

After introducing equation (3-10) into (3-9), rearrangement yields

$$\gamma M^2 = 7 \left(\frac{\Theta_v}{\Theta_{v0}} - 1 \right) + 2\delta\Theta_v (\coth \Theta_{v0} - \coth \Theta_v) \quad (3-11)$$

4. TAYLOR-MACCOLL FLOW

In this chapter, we develop the equations governing Taylor-Maccoll flow. The nomenclature is indicated in figure 1

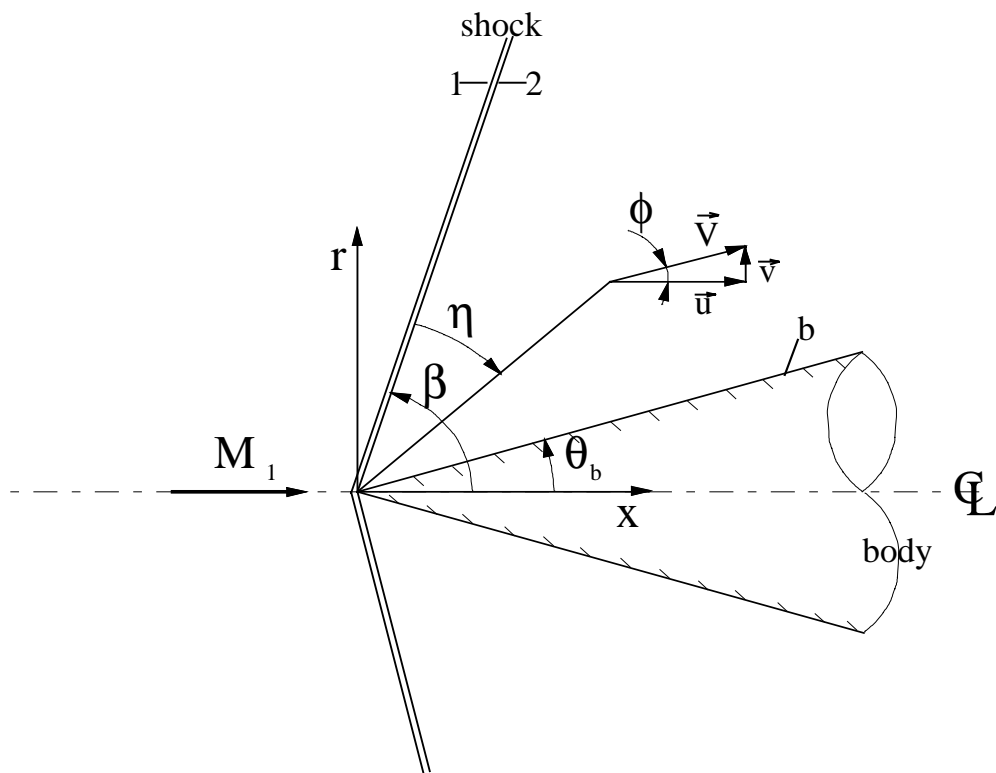


Figure 1 Nomenclature for Taylor-Maccoll flow

As the sketch hints, the shock is conical and attached to the apex of the body if the semi-vertex angle θ_b is not too large. The streamline angle ϕ is measured relative to the centerline. This streamline angle starts as ϕ_2 right behind the shock and increases to $\phi_b = \theta_b$ at the body.

In the computation, we first calculate conditions behind the shock and then proceed to the body. Therefore, we first derive the relations for the shock.

4.1 SHOCK DYNAMICS

In this chapter, we provide the equations necessary to determine conditions right behind the shock for a given shock angle β , upstream Mach number M_1 , and nondimensional stagnation temperature Θ_{v0} . The shock itself can be treated as a planar oblique shock, because a ray along a conical shock is straight when it passes through the cone's vertex. In the coming derivation, we use the nomenclature indicated in figure 2. In the case of a planar wedge, one would have to replace the

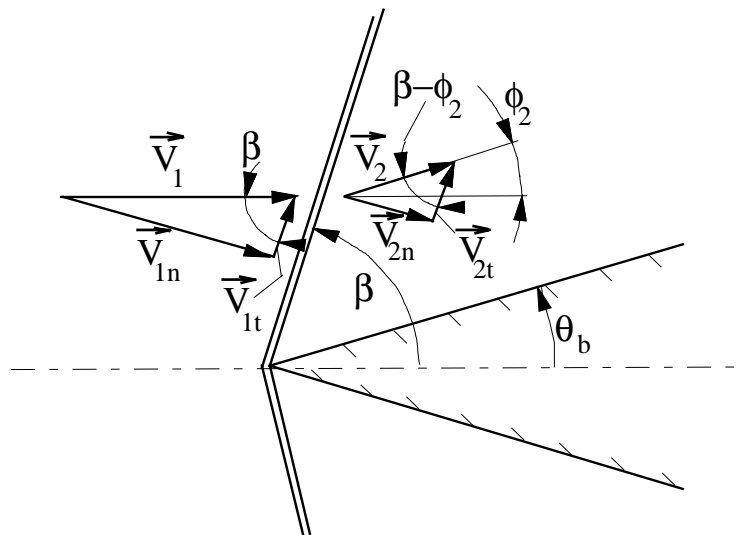


Figure 2 Nomenclature for shock

streamline angle right behind the shock ϕ_2 with the planar semi-vertex angle θ_b . Some relations are easy to obtain from the sketch

$$V_{1n} = V_1 \sin\beta = V_{1t} \tan\beta \quad (4-1)$$

$$V_{2n} = V_2 \sin(\beta - \phi_2) = V_{2t} \tan(\beta - \phi_2) \quad (4-2)$$

Furthermore, we need the following relations

$$M_{1n} = M_1 \sin\beta = M_{1t} \tan\beta \quad (4-3)$$

$$M_{2n} = M_2 \sin(\beta - \phi_2) = M_{2t} \tan(\beta - \phi_2) \quad (4-4)$$

$$M_{1n} = \frac{V_{1n}}{a_1} \quad (4-5)$$

$$M_{2n} = \frac{V_{2n}}{a_2} \quad (4-6)$$

The usual jump conditions for an oblique shock, resulting from conservation of mass, momentum, and energy, are⁶

$$(\rho V_n)_1 = (\rho V_n)_2 \quad (4-7)$$

$$(p + \rho V_n^2)_1 = (p + \rho V_n^2)_2 \quad (4-8)$$

$$\left(h + \frac{1}{2} V_n^2 \right)_1 = \left(h + \frac{1}{2} V_n^2 \right)_2 \quad (4-9)$$

From preservation of the tangential momentum, we have

$$V_{t1} = V_{t2} \quad (4-10)$$

Equations (4-7)-(4-10) are independent of the gas model, and are therefore valid for perfect and imperfect gases. Rewrite equation (4-7) as

$$\frac{\rho_2}{\rho_1} = \frac{V_{1n}}{V_{2n}} \quad (4-11)$$

Thus, equation (4-8) may be rearranged to

$$p_2 = p_1 + \rho_1 V_{1n}^2 \left(1 - \frac{V_{2n}}{V_{1n}} \right) \quad (4-12)$$

Introduce equations (2-1) and (2-12) into (4-12)

$$\rho_2 R_g T_2 = \rho_1 R_g T_1 + \rho_1 \gamma_1 R_g T_1 M_1^2 \left(1 - \frac{V_{2n}}{V_{1n}} \right) \quad (4-13)$$

After substituting equation (4-11) into equation (4-13), it follows

$$\frac{V_{1n} T_2}{V_{2n} T_1} = 1 + \gamma_1 M_1^2 \left(1 - \frac{V_{2n}}{V_{1n}} \right) \quad (4-14)$$

Replacing the normal velocities with equation (3-7) and rearranging lead to

$$\frac{\Theta_{v2}}{\Theta_{v1}} = \frac{\gamma_1 M_{1n}^2 \left(1 + \gamma_2 M_{2n}^2 \right)}{\gamma_2 M_{2n}^2 \left(1 + \gamma_1 M_{1n}^2 \right)} \quad (4-15)$$

Equation (4-15) can be rewritten with equations (2-1) and (4-11), thus yielding

$$\frac{\rho_2}{\rho_1} = \frac{V_{1n}}{V_{2n}} = \frac{\gamma_1 M_{1n}^2 \left(1 + \gamma_2 M_{2n}^2 \right)}{\gamma_2 M_{2n}^2 \left(1 + \gamma_1 M_{1n}^2 \right)} \quad (4-16)$$

$$\frac{p_2}{p_1} = \frac{1 + \gamma_1 M_{1n}^2}{1 + \gamma_2 M_{2n}^2} \quad (4-17)$$

Equations (4-15), (4-16), and (4-17) represent the jump conditions across the shock in terms of γ_1 , γ_2 , M_{1n} , and M_{2n} . They hold for perfect and imperfect gases.

To determine M_{2n} , we may use for a perfect gas the standard oblique shock relation, while for the imperfect gas an iterative procedure has to be employed. This procedure will be explained in chapter 5. For a perfect gas, we use⁷

$$\delta = 0 \Rightarrow M_{2n} = \sqrt{\frac{1 + \frac{\gamma-1}{2} M_{1n}^2}{\gamma M_{1n}^2 - \frac{\gamma-1}{2}}} \quad (4-18)$$

In the following, we establish equations expressing the relation between the shock angle β and the streamline angle right behind the shock ϕ_2 . For a perfect gas, the standard oblique shock relations can be used⁶

$$\delta = 0 \Rightarrow \tan \phi_2 = \frac{\cot \beta (M_1^2 \sin^2 \beta - 1)}{1 + ((\gamma+1)/2 - \sin^2 \beta) M_1^2} \quad (4-19)$$

The counterpart for an imperfect gas is derived from equation (4-16) using equations (4-1), (4-2), and (4-10)

$$\delta = 1 \Rightarrow \frac{\tan \beta}{\tan(\beta - \phi_2)} = \frac{\gamma_1 M_{1n}^2 \left(\frac{1 + \gamma_2 M_{2n}^2}{1 + \gamma_1 M_{1n}^2} \right)^2}{\gamma_2 M_{2n}^2} \quad (4-20)$$

Simple rearrangement and employing equation (4-3) yield

$$\delta = 1 \Rightarrow \phi_2 = \beta - \tan^{-1} \left(\frac{\gamma_2 M_{2n}^2 (1 + \gamma_1 M_1^2 \sin^2 \beta)}{\gamma_1 M_1^2 \sin \beta \cos \beta (1 + \gamma_2 M_{2n}^2)} \right) \quad (4-21)$$

Next, we derive an equation that utilizes equation (4-9). For this, we choose the convenient reference state

$$T_r = T_v \quad \text{and} \quad e_r = \frac{R_g T_v}{2} \left(5 + \delta \coth \frac{1}{2} \right) \quad (4-22)$$

and introduce this reference state into equation (2-16), thus yielding

$$e(T) = \frac{RT_v}{2} \left(\frac{5}{2\Theta_v} + \delta \coth \Theta_v \right) \quad (4-23)$$

Substituting equation (4-23) into equation (3-8), results in

$$h_0 = \frac{RT_v}{4\Theta_v} (7 + 2\delta\Theta_v \coth \Theta_v + \gamma M^2) \quad (4-24)$$

Equation (4-24) may be written for the upstream side of the shock, as well as for the downstream side of the shock

$$h_{01} = \frac{RT_v}{4} \frac{1}{\Theta_{v1}} (7 + 2\delta\Theta_{v1} \coth \Theta_{v1} + \gamma_1 M_{1n}^2) \quad (4-25)$$

$$h_{02} = \frac{RT_v}{4} \frac{1}{\Theta_{v2}} (7 + 2\delta\Theta_{v2} \coth \Theta_{v2} + \gamma_2 M_{2n}^2) \quad (4-26)$$

With $h_{01} = h_{02}$ it follows that

$$\Theta_{v2} = \Theta_{v1} \left(\frac{7 + \gamma_2 M_{2n}^2 + 2\delta \Theta_{v2} \coth \Theta_{v2}}{7 + \gamma_1 M_{1n}^2 + 2\delta \Theta_{v1} \coth \Theta_{v1}} \right) \quad (4-27)$$

This equation will later be employed in an iterative procedure, since it is an implicit equation for the imperfect gas case.

As the last topic, we derive the minimum possible shock angle β_{\min} . Because of symmetry, $\phi_2=0$ is the smallest possible streamline angle. From equation (4-19) for the $\delta=0$ case

$$0 = \frac{\cot \beta_{\min} (M_1^2 \sin^2 \beta_{\min} - 1)}{1 + \left(\frac{\gamma + 1}{2} - \sin^2 \beta_{\min} \right) M_1^2} \quad (4-28)$$

we have

$$M_1^2 \sin^2 \beta_{\min} - 1 = 0 \quad (4-30)$$

Equation (4-30) yields

$$\beta_{\min} = \sin^{-1} \frac{1}{M_1} \quad (4-31)$$

One can see that β_{\min} equals the Mach angle μ . β_{\min} does not depend on the ratio of specific heats γ . Therefore, equation (4-31) is also valid for the imperfect gas case.

4.2 FLOW FIELD BETWEEN SHOCK AND BODY

In this chapter, we derive the differential equations governing the flow field between shock and body. The flow is inviscid, steady, without swirl, without body forces, and axisymmetric. The reader will find the coordinate system in figure 1 (page 10). The \hat{e}_ψ -direction is perpendicular to the r- and x-directions. Thus, the gradient operator becomes

$$\nabla = \hat{e}_r \frac{\partial}{\partial r} + \hat{e}_\psi \frac{1}{r} \frac{\partial}{\partial \psi} + \hat{e}_x \frac{\partial}{\partial x} \quad (4-32)$$

Derivatives of the unit vectors are

$$\frac{\partial \hat{e}_i}{\partial q_j} = 0 \quad \text{for } \begin{cases} i = 1, 2, 3 \\ j = 1, 2, 3 \end{cases} \quad \text{except: } \frac{\partial \hat{e}_r}{\partial \psi} = \hat{e}_\psi \quad \text{and} \quad \frac{\partial \hat{e}_\psi}{\partial \psi} = -\hat{e}_r \quad (4-33)$$

Furthermore, it is worth noting that the derivatives of all quantities with respect to ψ are zero, except for the ones above. For the velocity, we can write

$$\vec{V} = v\hat{e}_r + u\hat{e}_x \quad (4-34)$$

Because the flow is steady, the substantial derivative may be written as

$$\frac{D}{Dt} = \frac{\partial}{\partial t} + \vec{V} \cdot \nabla = \vec{V} \cdot \nabla \quad (4-35)$$

The continuity equation is

$$\begin{aligned}\frac{D\rho}{Dt} + \rho \nabla \cdot \vec{V} &= 0 \\ \vec{V} \cdot \nabla \rho + \rho \nabla \cdot \vec{V} &= 0 \\ \nabla \cdot (\rho \vec{V}) &= 0\end{aligned}\tag{4-36}$$

which becomes

$$\frac{\partial(r\rho v)}{\partial r} + r \frac{\partial(\rho u)}{\partial x} = 0\tag{4-37}$$

The Euler momentum equation in the x-direction is

$$\frac{Du}{Dt} + \frac{1}{\rho} \frac{\partial p}{\partial x} = 0\tag{4-38}$$

We introduce (4-35) and (4-36) into (4-38), which yields

$$v \frac{\partial u}{\partial r} + u \frac{\partial u}{\partial x} + \frac{1}{\rho} \frac{\partial p}{\partial x} = 0\tag{4-39}$$

One can show, using Crocco's equation, that the scalar vorticity is zero

$$\omega = \frac{\partial v}{\partial x} - \frac{\partial u}{\partial r} = 0\tag{4-40}$$

Taylor-Maccoll flow doesn't have any intrinsic length scale and we may therefore seek a similarity solution. This means that flow conditions only depend on the angle η . Hence, we introduce new independent variables ξ and η , as follows

$$\begin{aligned}\xi &= x \\ \eta &= \beta - \tan^{-1} \frac{r}{x}\end{aligned}\tag{4-41}$$

One can see that the angle η is measured from the shock inward. The pressure, density, and velocity components depend only on the angle η and can be expressed as

$$\begin{aligned}p &= p_2 P(\eta) \\ \rho &= \rho_2 R(\eta) \\ u &= V_2 Q(\eta) \cos \phi(\eta) \\ v &= V_2 Q(\eta) \sin \phi(\eta)\end{aligned}\tag{4-42}$$

As usual, the subscript 2 denotes a location right behind the shock. Initial conditions at station 2, where $\eta=0$, are

$$\begin{aligned}P(0) &= Q(0) = R(0) = 1 \\ \phi(0) &= \phi_2\end{aligned}\tag{4-43}$$

The tangency condition at the body is

$$\phi(\beta - \theta_b) = \theta_b\tag{4-44}$$

The goal of the following derivation is to provide an expression for the Mach number in terms of the new variables. The speed of sound is

$$a^2 = \gamma \frac{p}{\rho}\tag{4-45}$$

thus, yielding for the Mach number

$$M^2 = \frac{V^2}{a^2} = \frac{V^2 \rho}{\gamma p} \quad (4-46)$$

which equals

$$M_2^2 = \frac{V_2^2 \rho_2}{\gamma_2 p_2} \quad (4-47)$$

just downstream of the shock. After introducing similarity variables, we have

$$M^2 = \frac{V_2^2 Q^2 \rho_2 R}{\gamma_2 P} = \frac{Q^2 R}{P} \frac{\gamma_2 V_2^2 \rho_2}{\gamma \gamma_2 p_2}$$

which becomes

$$M^2 = \frac{Q^2 R}{P} \frac{\gamma_2}{\gamma} M_2^2 \quad (4-48)$$

We now determine derivatives in terms of the new coordinates

$$\frac{\partial}{\partial r} = \frac{\partial \xi}{\partial r} \frac{\partial}{\partial \xi} + \frac{\partial \eta}{\partial r} \frac{\partial}{\partial \eta} = \frac{\partial x}{\partial r} \frac{\partial}{\partial \xi} + \frac{\partial(\beta - \tan^{-1} r/x)}{\partial r} \frac{\partial}{\partial \eta}$$

$$\frac{\partial}{\partial r} = -\frac{\cos^2(\beta - \eta)}{\xi} \frac{\partial}{\partial \eta} \quad (4-49)$$

$$\frac{\partial}{\partial x} = \frac{\partial \xi}{\partial x} \frac{\partial}{\partial \xi} + \frac{\partial \eta}{\partial x} \frac{\partial}{\partial \eta} = \frac{\partial x}{\partial x} \frac{\partial}{\partial \xi} + \frac{\partial(\beta - \tan^{-1} r/x)}{\partial x} \frac{\partial}{\partial \eta}$$

$$\frac{\partial}{\partial x} = \frac{\partial}{\partial \xi} + \frac{\sin(\beta - \eta) \cos(\beta - \eta)}{\xi} \frac{\partial}{\partial \eta} \quad (4-50)$$

With equations (4-42), (4-49), and (4-50), the continuity equation (4-41) becomes

$$\begin{aligned}
& -\frac{\cos^2(\beta-\eta)}{\xi} \frac{\partial}{\partial \eta} \{ \xi \tan(\beta-\eta) \rho_2 R(\eta) V_2 Q(\eta) \sin \phi(\eta) \} + \\
& + \xi \tan(\beta-\eta) \frac{\partial}{\partial \xi} \{ \rho_2 R(\eta) V_2 Q(\eta) \cos \phi(\eta) \} + \\
& + \xi \tan(\beta-\eta) \frac{\sin(\beta-\eta) \cos(\beta-\eta)}{\xi} \frac{\partial}{\partial \eta} \{ \rho_2 R(\eta) V_2 Q(\eta) \cos \phi(\eta) \} = 0
\end{aligned}$$

In this equation, we made use of an expression for r that stems directly from equations (4-37)

$$r = \xi \tan(\beta - \eta)$$

Simplification and several cancellations result in a convenient form for the continuity equation

$$\sin(\beta - \eta) \tan(\beta - \eta) \{ R Q \cos \phi \}' - \cos(\beta - \eta) \{ \tan(\beta - \eta) R Q \sin \phi \}' = 0 \quad (4-51)$$

where $\frac{\partial}{\partial \eta} = \{ \dots \}'$

We introduce the new coordinates into the momentum equation, to obtain

$$\begin{aligned}
& V_2 Q \sin \phi \left(-\frac{\cos^2(\beta-\eta)}{\xi} \right) \frac{\partial}{\partial \eta} \{ V_2 Q(\eta) \cos \phi(\eta) \} + \\
& + V_2 Q \cos \phi \left(\frac{\sin(\beta-\eta) \cos(\beta-\eta)}{\xi} \right) \frac{\partial}{\partial \eta} \{ V_2 Q(\eta) \cos \phi(\eta) \} + \\
& + \frac{1}{\rho_2 R} \left(\frac{\sin(\beta-\eta) \cos(\beta-\eta)}{\xi} \right) \frac{\partial}{\partial \eta} \{ p_2 P(\eta) \} = 0
\end{aligned}$$

Note that derivatives with respect to ξ are zero. The above equation may be rearranged to

$$\frac{V_2^2 \rho_2}{p_2} R Q \sin(\beta - \eta - \phi) \{Q \cos \phi\}' + \sin(\beta - \eta) P' = 0 \quad (4-52)$$

It is still necessary to derive a convenient form of the vorticity equation (4-40) in terms of the new variables. With equations (4-41), (4-42), (4-49), and (4-50), equation (4-40) becomes

$$\begin{aligned} & \frac{\sin(\beta - \eta) \cos(\beta - \eta)}{\xi} \frac{\partial}{\partial \eta} \{V_2 Q(\eta) \sin \phi(\eta)\} + \\ & + \frac{\cos^2(\beta - \eta)}{\xi} \frac{\partial}{\partial \eta} \{V_2 Q(\eta) \cos \phi(\eta)\} = 0 \end{aligned}$$

Rearrangement yields for the vorticity equation

$$\sin(\beta - \eta) \{Q \sin \phi\}' + \cos(\beta - \eta) \{Q \cos \phi\}' = 0 \quad (4-53)$$

We next arrange the equations so they become suitable for computer use. First, we rearrange the vorticity equation (4-53) as follows

$$\begin{aligned} & \sin(\beta - \eta) [Q' \sin \phi + Q \phi' \cos \phi] + \cos(\beta - \eta) [Q' \cos \phi - Q \phi' \sin \phi] = 0 \\ & [\sin(\beta - \eta) \sin \phi + \cos(\beta - \eta) \cos \phi] Q' + [\sin(\beta - \eta) \cos \phi - \cos(\beta - \eta) \sin \phi] Q \phi' = 0 \\ & \cos(\beta - \eta - \phi) Q' + \sin(\beta - \eta - \phi) Q \phi' = 0 \end{aligned}$$

thus, yielding

$$\frac{Q'}{Q} = -\phi' \tan(\beta - \eta - \phi) \quad (4-54)$$

Introduce equations (4-47) and (4-48) into the momentum equation (4-52), resulting in

$$\frac{M^2 \gamma P}{Q^2 R} R Q \sin(\beta - \eta - \phi) [Q' \cos \phi - Q \phi' \sin \phi] + \sin(\beta - \eta) P' = 0$$

$$M^2 \gamma \sin(\beta - \eta - \phi) \left[\frac{Q'}{Q} \cos \phi - \phi' \sin \phi \right] + \sin(\beta - \eta) \frac{P'}{P} = 0$$

Replace ϕ' with equation (4-54) and simplify

$$M^2 \gamma \sin(\beta - \eta - \phi) \left[\frac{Q'}{Q} \cos \phi + \frac{Q'}{Q} \sin \phi \cot(\beta - \eta - \phi) \right] + \sin(\beta - \eta) \frac{P'}{P} = 0$$

$$M^2 \gamma \frac{Q'}{Q} [\sin(\beta - \eta - \phi) \cos \phi + \sin \phi \cos(\beta - \eta - \phi)] = -\sin(\beta - \eta) \frac{P'}{P}$$

$$M^2 \gamma \frac{Q'}{Q} [\sin(\beta - \eta)] = -\sin(\beta - \eta) \frac{P'}{P}$$

to obtain

$$\frac{P'}{P} = -\gamma M^2 \frac{Q'}{Q} \quad (4-55)$$

We rearrange the continuity equation (4-51) as

$$\sin^2(\beta - \eta) R' Q \cos \phi + \sin^2(\beta - \eta) R Q' \cos \phi - \sin^2(\beta - \eta) R Q \phi' \sin \phi +$$

$$+ R Q \sin \phi - \cos(\beta - \eta) \sin(\beta - \eta) R' Q \sin \phi +$$

$$- \cos(\beta - \eta) \sin(\beta - \eta) R Q' \sin \phi - \cos(\beta - \eta) \sin(\beta - \eta) R Q \phi' \cos \phi = 0$$

which simplifies to

$$\frac{R'}{R} \sin(\beta - \eta) \sin(\beta - \eta - \phi) + \frac{Q'}{Q} \sin(\beta - \eta) \sin(\beta - \eta - \phi) + \sin \phi =$$

$$= \phi' \sin(\beta - \eta) \cos(\beta - \eta - \phi)$$

Introduce equation (4-54), multiply by $\cos(\beta - \eta - \phi)$, and simplify, to obtain

$$\frac{R'}{R} \sin(\beta - \eta - \phi) \cos(\beta - \eta - \phi) + \frac{\sin \phi \cos(\beta - \eta - \phi)}{\sin(\beta - \eta)} = \phi'$$

$$\frac{R'}{R} = \frac{\phi'}{\sin(\beta - \eta - \phi) \cos(\beta - \eta - \phi)} - \frac{\sin \phi}{\sin(\beta - \eta) \sin(\beta - \eta - \phi)} \quad (4-56)$$

4.2.1 PERFECT GAS

In this and the next chapter, we develop a convenient equation for ϕ' . It would be difficult to do this in a general way (e.g., for both $\delta=0$ and $\delta=1$), which is why we derive these equations separately. We start with $\delta=0$.

Before we can simplify equations (4-54)-(4-56), we need the relation between pressure and density for a homentropic flow⁶

$$\frac{p}{p_0} = \left(\frac{\rho}{\rho_0} \right)^\gamma \quad (4-57)$$

or

$$P = R^\gamma \quad (4-58)$$

We insert equation (4-48) into equation (4-55), resulting in

$$P' = -\gamma M_2^2 R Q Q' \quad (4-59)$$

We already made use of $\gamma_2 = \gamma = \text{const.}$ for the perfect gas. R may be replaced in equation (4-59) with equation (4-58)

$$P' = -\gamma M_2^2 P^{\frac{1}{\gamma}} Q Q' \quad (4-60)$$

which results in

$$P^{-\frac{1}{\gamma}} \frac{dP}{d\eta} = -\gamma M_2^2 Q \frac{dQ}{d\eta} \quad (4-61)$$

and integrates to

$$\frac{\gamma}{\gamma-1} P^{\frac{\gamma-1}{\gamma}} = -\gamma M_2^2 \frac{Q^2}{2} + \text{const.} \quad (4-62)$$

The constant of integration is determined with the initial conditions right behind the shock, equations (4-43). Simplification leads to

$$P = \left(1 + \frac{\gamma-1}{2} M_2^2 (1-Q^2)\right)^{\frac{\gamma}{\gamma-1}} \quad (4-63)$$

P may be replaced in equation (4-63) with equation (4-58), resulting in

$$R = \left(1 + \frac{\gamma-1}{2} M_2^2 (1-Q^2)\right)^{\frac{1}{\gamma-1}} \quad (4-64)$$

Equation (4-64) enables us to combine equations (4-54) and (4-56), thus, eliminating derivatives of all properties except ϕ . First, we take the derivative of equation (4-64)

$$R' = -\left(1 + \frac{\gamma-1}{2} M_2^2 (1-Q^2)\right)^{\frac{2-\gamma}{\gamma-1}} M_2^2 Q Q' \quad (4-65)$$

Divide equation (4-65) by (4-64) to obtain

$$\frac{R'}{R} = -\frac{M_2^2 Q}{\left(1 + \frac{\gamma-1}{2} M_2^2 (1-Q^2)\right)} Q' \quad (4-66)$$

We eliminate Q' from equation (4-66) with equation (4-54), leading to:

$$\frac{R'}{R} = \frac{M_2^2 Q^2 \phi' \tan(\beta - \eta - \phi)}{\left(1 + \frac{\gamma-1}{2} M_2^2 (1-Q^2)\right)} \quad (4-67)$$

Finally, we set equation (4-67) equal to equation (4-56) and solve for ϕ' , thereby resulting in the desired equation

$$\phi' = \frac{\sin \phi \cos(\beta - \eta - \phi)}{\sin(\beta - \eta) \left(1 - \frac{M_2^2 Q^2 \sin^2(\beta - \eta - \phi)}{1 + \frac{\gamma - 1}{2} M_2^2 (1 - Q^2)} \right)} \quad (4-68)$$

This relation is numerically integrated in conjunction with equation (4-54).

4.2.2 IMPERFECT GAS

The imperfect gas counterpart to the homentropic relation (4-57) gas may be obtained from equation (3-3). Equation (3-3) is written with conditions at station 2 as the reference state, with the result

$$\frac{\rho}{\rho_2} = \left(\frac{\Theta_{v2}}{\Theta_v} \right)^{\frac{5}{2}} \left(\frac{\sinh \Theta_{v2}}{\sinh \Theta_v} \right)^{\delta} \exp[\delta(\Theta_v \coth \Theta_v - \Theta_{v2} \coth \Theta_{v2})] \quad (4-69)$$

Introduce similarity variables (4-42) and $\delta=1$, to obtain

$$R = \left(\frac{\Theta_{v2}}{\Theta_v} \right)^{\frac{5}{2}} \left(\frac{\sinh \Theta_{v2}}{\sinh \Theta_v} \right) \exp(\Theta_v \coth \Theta_v - \Theta_{v2} \coth \Theta_{v2}) \quad (4-70)$$

With equation (4-70) and the thermal equation of state, we find an expression for P. First, similarity variables are introduced into the equation of state (2-1)

$$\begin{aligned}
\frac{P}{\rho T} &= R_g \\
\frac{P}{\rho T} &= \frac{p_2}{\rho_2 T_2} \\
\frac{p_2 P(\eta)}{\rho_2 R(\eta) T} &= \frac{p_2}{\rho_2 T_2} \\
P &= R \frac{T}{T_2} = R \frac{\Theta_{v2}}{\Theta_v} \tag{4-71}
\end{aligned}$$

We combine equations (4-70) and (4-71)

$$P = \left(\frac{\Theta_{v2}}{\Theta_v} \right)^{\frac{7}{2}} \left(\frac{\sinh \Theta_{v2}}{\sinh \Theta_v} \right) \exp(\Theta_v \coth \Theta_v - \Theta_{v2} \coth \Theta_{v2}) \tag{4-72}$$

Rewrite and take the derivative of equation (4-70), to result in

$$\begin{aligned}
R &= \Theta_{v2}^{\frac{5}{2}} \sinh \Theta_{v2} \exp(-\Theta_{v2} \coth \Theta_{v2}) \left[\Theta_v^{\frac{5}{2}} \sinh^{-1} \Theta_v \exp(\Theta_v \coth \Theta_v) \right] \\
R' &= \Theta_{v2}^{\frac{5}{2}} \sinh \Theta_{v2} \exp(-\Theta_{v2} \coth \Theta_{v2}) \left[-\frac{5 \Theta_v' \exp(\Theta_v \coth \Theta_v)}{2 \Theta_v^{\frac{7}{2}} \sinh \Theta_v} + \right. \text{After} \\
&\quad \left. - \frac{\Theta_v' \cosh \Theta_v \exp(\Theta_v \coth \Theta_v)}{\Theta_v^{\frac{5}{2}} \sinh^2 \Theta_v} + \frac{\Theta_v' \left(\coth \Theta_v - \frac{\Theta_v}{\sinh^2 \Theta_v} \right) \exp(\Theta_v \coth \Theta_v)}{\Theta_v^{\frac{5}{2}} \sinh^2 \Theta_v} \right]
\end{aligned}$$

dividing R' by R and several cancellations, we have

$$\frac{R'}{R} = -\frac{1}{2} \left[5 + 2 \left(\frac{\Theta_v}{\sinh \Theta_v} \right)^2 \right] \frac{\Theta_v'}{\Theta_v} \tag{4-73}$$

Applying the same procedure to equation (4-72) leads to

$$\frac{P'}{P} = -\frac{1}{2} \left[7 + 2 \left(\frac{\Theta_v}{\sinh \Theta_v} \right)^2 \right] \frac{\Theta'_v}{\Theta_v} \quad (4-74)$$

By combining equations (4-54) and (4-55), we have

$$\frac{P'}{P} = \gamma M^2 \phi' \tan(\beta - \eta - \phi) \quad (4-75)$$

Set equation (4-74) equal to equation (4-75), to obtain the desired equation for ϕ'

$$\phi' = -\frac{1}{2} \frac{7 + 2 \left(\frac{\Theta_v}{\sinh \Theta_v} \right)^2}{\gamma M^2 \tan(\beta - \eta - \phi)} \frac{\Theta'_v}{\Theta_v} \quad (4-76)$$

Finally, we derive an expression for $\frac{\Theta'_v}{\Theta_v}$. By combining equations (4-56) and (4-73) and replacing ϕ' with equation (4-76), we have

$$\frac{1}{2} \frac{\Theta'_v}{\Theta_v} \left[5 + 2 \left(\frac{\Theta_v}{\sinh \Theta_v} \right)^2 - \frac{7 + 2 \left(\frac{\Theta_v}{\sinh \Theta_v} \right)^2}{\gamma M^2 \sin^2(\beta - \eta - \phi)} \right] = \frac{\sin \phi}{\sin(\beta - \eta - \phi) \sin(\beta - \eta)} \quad (4-77)$$

Substitute equation (2-11) and rearrange to obtain the equation we were looking for

$$\frac{\Theta'_v}{\Theta_v} = \frac{2M^2 \sin(\beta - \eta - \phi) \sin \phi}{\left[5 + 2 \left(\frac{\Theta_v}{\sinh \Theta_v} \right)^2 \right] \sin(\beta - \eta) [M^2 \sin^2(\beta - \eta - \phi) - 1]} \quad (4-78)$$

4.3 SURFACE PRESSURE COEFFICIENT C_{pb}

The surface pressure coefficient C_{pb} is a parameter of great interest. With the help of C_{pb} , one can determine the pressure forces acting on the body

$$F_b = C_{pb} \frac{\rho_1}{2} V_1^2 A \quad (4-79)$$

where A denotes the projected frontal area of the cone and

$$C_{pb} = \frac{p_b - p_1}{\frac{\rho_1}{2} V_1^2} \quad (4-80)$$

With equations (2-1), (2-7), (4-42), and (3-5) we can write for equation (4-80)

$$C_{pb} = \frac{2\left(\frac{p_b}{p_1} - 1\right)}{\gamma_1 M_1^2} = \frac{2\left(\frac{p_2}{p_1} P(\eta_b) - 1\right)}{\gamma_1 M_1^2} \quad (4-81)$$

5. COMPUTER PROCEDURE

In this chapter, we describe the employed computer procedures. All computations are done in FORTRAN 77 with double precision. Here we point out the general process. We also explain equations that are used, numerical procedures, and error limits.

As mentioned in the introduction, the upstream Mach number, stagnation temperature Θ_{v0} , and the semi-vertex angle are prescribed. As the next step, we assume a shock angle β , determine conditions behind the shock, and integrate from the shock to the body. This gives us a streamline angle at the body. We then vary the shock angle β until the streamline angle at the body matches the semi-vertex angle (tangency condition).

We often need to determine the nondimensional temperature Θ_v and the ratio of specific heats γ . For this purpose, a subroutine 'thetav', detailed on the next page, is used.

Before starting the integration from the shock to the body, we need a subroutine that computes the properties right behind the shock for a given shock angle β . This subroutine is also used to calculate the dependence between the shock angle β and the semi-vertex angle θ_b (ϕ_2 for Taylor-Maccoll flow) for a plane wedge. We call this subroutine 'shock' and its description is on page 33. In order to get the β - θ_b plot, we vary β between β_{min} (from equation (4-31)) and 90° .

We make use of the notation ' \Leftarrow ' in the description of the subroutines. It means that the expression to the right of it becomes

stored under the variable to the left of it. This symbol is employed only in iteration loops. The ' \Leftarrow ' notation is now common practice and used, for example in reference 8.

subroutine thetav
input variables: δ , M , and Θ_{v0}
employed procedure: for $\delta=0$ $\gamma = \frac{7}{5}$ $\Theta_v = \Theta_{v0} \left(1 + \frac{1}{5} M^2 \right) \quad \text{(from equation (3-11))}$ for $\delta=1$ - perform $\delta=0$ procedure and use this Θ_v as the starting value - repeat until relative difference between old and new values for Θ_v is less than 1.E-10 $\gamma \Leftarrow \left[7 + 2 \left(\frac{\Theta_v}{\sinh \Theta_v} \right)^2 \right] / \left[5 + 2 \left(\frac{\Theta_v}{\sinh \Theta_v} \right)^2 \right] \quad (2-11)$ $\Theta_v \Leftarrow \Theta_{v0} \left[1 + \frac{1}{7} \left\{ \gamma M^2 + 2 \Theta_v (\coth \Theta_v - \coth \Theta_{v0}) \right\} \right]$ <div style="text-align: right;">(3-11)</div>
output variables: Θ_v and γ

subroutine shock	
input variables: β, δ, M_1 , and Θ_{v0}	
employed procedure:	
- calculate γ_1 and Θ_{v1} with thetav	
for $\delta=0$	
$M_{1n} = M_1 \sin \beta$ (4-3)	
$M_{2n} = \sqrt{\left(1 + \frac{\gamma_1 - 1}{2} M_{1n}^2\right) / \left(\gamma_1 M_{1n}^2 - \frac{\gamma_1 - 1}{2}\right)}$ (4-18)	
$\gamma_2 = \frac{7}{5}$ (2-11)	
$\Theta_{v2} = \Theta_{v1} \left[\frac{7 + \gamma_2 M_{2n}^2}{7 + \gamma_1 M_{1n}^2} \right]$ (4-27)	
$\phi_2 = \tan^{-1} \left[\frac{\{(M_{1n}^2 - 1) \cot \beta\}}{\left\{1 + \left(\frac{\gamma_1 + 1}{2} - \sin^2 \beta\right) M_1^2\right\}} \right]$	
$M_2 = M_{2n} / \sin(\beta - \phi_2)$ (4-4) (4-19)	
for $\delta=1$	
- perform $\delta=0$ procedure and use:	
- M_{1n} as final result also for $\delta=1$	
- $M_{2n}, \Theta_{v2}, \gamma_2$, and ϕ_2 as iteration start values	
- repeat until relative difference between old values and new values for Θ_{v2} and also for M_{2n} is less than 1.E-10	
$\Theta_{v2} \Leftarrow \Theta_{v1} \left(\frac{7 + \gamma_2 M_{2n}^2 + 2\Theta_{v2} \coth \Theta_{v2}}{7 + \gamma_1 M_{1n}^2 + 2\Theta_{v1} \coth \Theta_{v1}} \right)$ (4-27)	
$\gamma_2 \Leftarrow \left[7 + 2 \left(\frac{\Theta_{v2}}{\sinh \Theta_{v2}} \right)^2 \right] / \left[5 + 2 \left(\frac{\Theta_{v2}}{\sinh \Theta_{v2}} \right)^2 \right]$	
$M_{2n} \Leftarrow \sqrt{\frac{M_{1n}^2 \gamma_1 \Theta_{v1}}{\gamma_2 \Theta_{v2}} \left(\frac{1 + \gamma_2 M_{2n}^2}{1 + \gamma_1 M_{1n}^2} \right)}$ (4-15) (2-11)	
$\phi_2 = \beta - \tan^{-1} \left(\frac{\gamma_2 M_{2n}^2 (1 + \gamma_1 M_{1n}^2)}{\gamma_1 M_1^2 \sin \beta \cos \beta (1 + \gamma_2 M_{2n}^2)} \right)$ (4-20)	
$M_2 = M_{2n} / \sin(\beta - \phi_2)$ (4-4)	
output variables: $\Theta_{v1}, \Theta_{v2}, \gamma_1, \gamma_2, M_2$, and ϕ_2	

Next, we discuss how we obtain the β - θ_b plot for Taylor-Maccoll flow. We make initial guesses for β , integrate to the body, and vary β until the streamline angle at the body ϕ_b equals the semi-vertex angle θ_b . The variation of β is a simple linear interpolation process. We calculate the streamline angle at the body ϕ_b for two initial guesses for β , namely β_1 and β_2 . This gives us two streamline angles at the body ϕ_{b1} and ϕ_{b2} . After this, we find the new value for β by the following linear formula

$$\beta_{new} = \beta_1 - \left(\frac{\theta_b - \phi_{b1}}{\phi_{b2} - \phi_{b1}} \right) (\beta_1 - \beta_2) \quad (5-1)$$

We repeat this process, using β_{new} and β_{old} instead of β_2 and β_1 and ϕ_{bnew} and ϕ_{bold} instead of ϕ_{b2} and ϕ_{b1} , until the flow is aligned with the body at the body to an accuracy of 0.5E-8 radian ($\sim 2.9E-7$ degrees).

Our differential equations have a strong solution and a weak solution. To find both, we use

$$\begin{aligned} \text{weak solution} & \begin{cases} \beta_1 = \beta_{\min} - 1^\circ \cdot \pi / 180^\circ \\ \beta_2 = \beta_{\min} + 5^\circ \cdot \pi / 180^\circ \end{cases} \\ \text{strong solution} & \begin{cases} \beta_1 = 88^\circ \cdot \pi / 180^\circ \\ \beta_2 = 85^\circ \cdot \pi / 180^\circ \end{cases} \end{aligned}$$

For the integration from the shock to the body, we use the Runge-Kutta method. The integrations from the shock to the body are in two subroutines, one for the perfect gas case and one for the imperfect gas case. The used stepsize $\Delta\eta$ is the same for both cases. It has to be small enough to ensure, that the error of the streamline angle

at the body is far smaller than the accuracy for which the streamline angle has to match the body angle. This is necessary to guarantee convergence of the routine. We use a constant stepsize of $\Delta\eta=1.0E-4$ radian ($\sim 5.E-3$ degrees) for $\eta < \beta - \theta_b$. Thus, η assumes values of

$$\eta = i\Delta\eta \quad (i = 0, 1, 2, 3, \dots) \text{ for } \eta < \beta - \theta_b .$$

After having proceeded to the largest multiple of $\Delta\eta$, less than $\beta - \theta_b$, we take a last step with the new step size

$$(\Delta\eta)_{\text{last step}} = (\beta - \theta_b) - \max(i\Delta\eta) .$$

This procedure has proven to reduce the number of β -iterations significantly and has a positive effect on the overall accuracy. The Runge-Kutta method has a global error of the order $(\Delta\eta)^4$. However, we use the original step size $\Delta\eta$ for the estimation of the error. Thus, the estimated integration error is

$$(\Delta\eta)^4 = 1.E-16 \text{ radian } (\sim 5.E-15 \text{ degrees})$$

The variation of the shock angle β is done by the main program. It also checks the tangency condition at the body as described on page 34. For the integration, we use the subroutines 'perfiter' for the perfect gas case and 'imperfit' for the imperfect gas case (pages 37 and 38). 'Perfiter' calculates also Q at the body, which is used to calculate other properties. The subroutine 'imperfit' determines also Θ_v at the body.

The general idea of the Runge-Kutta method is as follows⁹

$$\begin{aligned}\vec{Y}_{i+1} &= \vec{Y}_i + h_i \left\{ \frac{1}{6} \vec{k}_1 + \frac{1}{3} \vec{k}_2 + \frac{1}{3} \vec{k}_3 + \frac{1}{6} \vec{k}_4 \right\} \\ \vec{k}_1 &= \vec{f}(x_i, \vec{Y}_i) \\ \vec{k}_2 &= \vec{f}\left\{x_i + h_i/2, (\vec{Y}_i + \vec{k}_1 h_i/2)\right\} \\ \vec{k}_3 &= \vec{f}\left\{x_i + h_i/2, (\vec{Y}_i + \vec{k}_2 h_i/2)\right\} \\ \vec{k}_4 &= \vec{f}\left\{x_i + h_i, (\vec{Y}_i + \vec{k}_3 h_i)\right\}\end{aligned}$$

(\vec{Y} dependent variables ; \vec{f} functions to integrate ; h_i stepsize)

In the computations, we use also the following equations, which are simple differentiating rules

$$\begin{aligned}\frac{Q'}{Q} &= (\ln Q)' \\ \frac{\Theta'_v}{\Theta_v} &= (\ln \Theta_v)'\end{aligned}$$

The Runge-Kutta method is utilized in subroutine 'imperfit' in a logarithmical form for Θ_v .

subroutine perfiter ($\delta=0$)
input variables: $M_1, \beta, \theta_b,$ and Θ_{v0}
external functions: $\phi'(\eta, \phi, \ln Q) = \frac{\sin \phi \cos(\beta - \eta - \phi)}{\sin(\beta - \eta) \left[1 - \frac{M_2^2 Q^2 \sin^2(\beta - \eta - \phi)}{1 + 0.2 M_2^2 \{1 - \exp(2 \ln Q)\}} \right]} \quad (4-68)$ $[\ln Q]'(\eta, \phi, \phi') = -\phi' \tan(\beta - \eta - \phi) \quad (4-54)$
employed procedure: <ul style="list-style-type: none"> - determine $\Theta_{v2}, M_2,$ and ϕ_2 with subroutine shock - set initial conditions $\phi = \phi_2, \ln Q = 0$ (for $Q = 1$), $\eta = 0$ - repeat as long as: $\eta < \beta - \theta_b$ with constant step size $\Delta\eta = 1.E-4$ - then use $(\Delta\eta)_{\text{last step}} = \theta_b - \max(i\Delta\eta)$ for last step $F1 \leftarrow \phi'(\eta, \phi, \ln Q)$ $G1 \leftarrow [\ln Q]'(\eta, \phi, F1)$ $F2 \leftarrow \phi' \left(\eta + \frac{\Delta\eta}{2}, \left(\phi + \frac{\Delta\eta}{2} F1 \right), \left(\ln Q + \frac{\Delta\eta}{2} G1 \right) \right)$ $G2 \leftarrow [\ln Q]' \left(\eta + \frac{\Delta\eta}{2}, \left(\phi + \frac{\Delta\eta}{2} F1 \right), F2 \right)$ $F3 \leftarrow \phi' \left(\eta + \frac{\Delta\eta}{2}, \left(\phi + \frac{\Delta\eta}{2} F2 \right), \left(\ln Q + \frac{\Delta\eta}{2} G2 \right) \right)$ $G3 \leftarrow [\ln Q]' \left(\eta + \frac{\Delta\eta}{2}, \left(\phi + \frac{\Delta\eta}{2} F2 \right), F3 \right)$ $F4 \leftarrow \phi'(\eta + \Delta\eta, (\phi + \Delta\eta F3), (\ln Q + \Delta\eta G3))$ $G4 \leftarrow [\ln Q]'(\eta + \Delta\eta, (\phi + \Delta\eta F3), F4)$ $\phi \leftarrow \phi + \Delta\eta (F1 + 2F2 + 2F3 + F4) / 6$ $\ln Q \leftarrow \ln Q + \Delta\eta (G1 + 2G2 + 2G3 + G4) / 6$ $\eta \leftarrow \eta + \Delta\eta$ $Q_b = \exp(\ln Q)$ $\phi_b = \phi$
output variables: ϕ_b and Q_b

subroutine imperfit ($\delta=1$)	
input variables:	$M_I, \beta, \theta_b,$ and Θ_{v0}
external functions:	(4-78)
	$[\ln \Theta_v]'(\eta, \phi, \Theta_v, M) = \frac{2M^2 \sin(\beta - \eta - \phi) \sin \phi}{[5 + 2(\Theta_v / \sinh \Theta_v)^2] \sin(\beta - \eta) [M^2 \sin^2(\beta - \eta - \phi) - 1]}$
	$\phi'(\eta, \phi, [\ln \Theta_v]', \Theta_v, M, \gamma) = -\frac{7 + 2(\Theta_v / \sinh \Theta_v)^2}{2\gamma M^2 \tan(\beta - \eta - \phi)} [\ln \Theta_v]' \quad (4-76)$
	$\gamma(\Theta_v) = [7 + 2(\Theta_v / \sinh \Theta_v)^2] / [5 + 2(\Theta_v / \sinh \Theta_v)^2] \quad (2-11)$
	$M(\Theta_v, \gamma) = \sqrt{[7(\Theta_v / \Theta_{v0} - 1) + 2\Theta_v (\coth \Theta_{v0} - \coth \Theta_v)] / \gamma} \quad (3-11)$
employed procedure:	
	<ul style="list-style-type: none"> - determine ϕ_2 and Θ_{v2} with subroutine shock - set initial conditions $\phi = \phi_2$, $\Theta_v = \Theta_{v2}$, and $\eta = 0$ - repeat as long as: $\eta < \beta - \theta_b$ with step size $\Delta\eta = 1.E-4$ - then use $(\Delta\eta)_{\text{last step}} = \theta_b - \max(i\Delta\eta)$ for last step
	$\gamma \leftarrow \gamma(\Theta_v)$
	$M \leftarrow M(\Theta_v, \gamma)$
	$F1 \leftarrow [\ln \Theta_v]'(\eta, \phi, \Theta_v, M)$
	$G1 \leftarrow \phi'(\eta, \phi, F1, \Theta_v, M, \gamma)$
	$\gamma \leftarrow \gamma(\Theta_v \exp(\frac{\Delta\eta}{2} F1))$
	$M \leftarrow M(\Theta_v \exp(\frac{\Delta\eta}{2} F1), \gamma)$
	$F2 \leftarrow [\ln \Theta_v]' \left(\left(\eta + \frac{\Delta\eta}{2} \right), \left(\phi + \frac{\Delta\eta}{2} G1 \right), \left(\Theta_v \exp(\frac{\Delta\eta}{2} F1) \right), M \right)$
	$G2 \leftarrow \phi' \left(\left(\eta + \frac{\Delta\eta}{2} \right), \left(\phi + \frac{\Delta\eta}{2} G1 \right), F2, \left(\Theta_v \exp(\frac{\Delta\eta}{2} F1) \right), M, \gamma \right)$
	$\gamma \leftarrow \gamma(\Theta_v \exp(\frac{\Delta\eta}{2} F2))$
	$M \leftarrow M(\Theta_v \exp(\frac{\Delta\eta}{2} F2), \gamma)$
	$F3 \leftarrow [\ln \Theta_v]' \left(\left(\eta + \frac{\Delta\eta}{2} \right), \left(\phi + \frac{\Delta\eta}{2} G2 \right), \left(\Theta_v \exp(\frac{\Delta\eta}{2} F2) \right), M \right)$

$G3 \leftarrow \phi \left(\left(\eta + \frac{\Delta\eta}{2} \right), \left(\phi + \frac{\Delta\eta}{2} G2 \right), F3, \left(\Theta_v \exp\left(\frac{\Delta\eta}{2} F2\right) \right), M, \gamma \right)$ $\gamma \leftarrow \gamma(\Theta_v \exp(\Delta\eta F3))$ $M \leftarrow M(\Theta_v \exp(\Delta\eta F3), \gamma)$ $F4 \leftarrow [\ln \Theta_v]' \left((\eta + \Delta\eta), (\phi + \Delta\eta G3), (\Theta_v \exp(\Delta\eta F3)), M \right)$ $G4 \leftarrow \phi' \left((\eta + \Delta\eta), (\phi + \Delta\eta G3), F4, (\Theta_v \exp(\Delta\eta F3)), M, \gamma \right)$ $\Theta_v \leftarrow \Theta_v \exp(\Delta\eta(F1 + 2F2 + 2F3 + F4)/6)$ $\phi \leftarrow \phi + \Delta\eta(G1 + 2G2 + 2G3 + G4)/6$ $\eta \leftarrow \eta + \Delta\eta$ $\Theta_{vb} = \Theta_v$ $\phi_b = \phi$
output variables: Θ_{vb} and ϕ_b

Up to this point, we have described how to compute:

$$M_2, \phi_2, \beta, Q_b \quad \text{for } \delta=0$$

$$\gamma_1, \gamma_2, M_2, \phi_2, \beta, \Theta_{v1}, \Theta_{v2}, \Theta_{vb} \quad \text{for } \delta=1$$

for prescribed values of M_1 , θ_b , and Θ_{v0} . For each set of prescribed conditions, we are able to calculate two sets of solutions, a strong solution and a weak solution. We also determine the ratios $\frac{M_{2 \delta=1}}{M_{2 \delta=0}}$ and $\frac{\beta_{\delta=1}}{\beta_{\delta=0}}$. Hence, we still have to compute M_b and C_{pb} and their imperfect to perfect gas ratios. The equations to determine C_{pb} and M_b for $\delta=0$ are

$$P_b = \left(1 + \frac{\gamma-1}{2} M_2^2 (1 - Q_b^2) \right)^{\frac{\gamma}{\gamma-1}} \quad (4-63)$$

$$\frac{p_2}{p_1} = \frac{1 + \gamma M_1^2 \sin^2 \beta}{1 + \gamma M_2^2 \sin^2 (\beta - \phi_2)} \quad (4-17)$$

Equation (4-81) is used for C_{pb}

$$\delta = 0 \Rightarrow C_{pb} = \frac{2 \left(\frac{p_2}{p_1} P_b - 1 \right)}{\gamma M_1^2}$$

Substitute equation (4-58) into equation (4-48) to yield

$$\delta = 0 \Rightarrow M_b = Q_b M_2 P_b^{\frac{1-\gamma}{2\gamma}}$$

For $\delta=1$ we compute

$$P_b = \left(\frac{\Theta_{v2}}{\Theta_{v0}} \right)^{\frac{7}{2}} \left(\frac{\sinh \Theta_{v2}}{\sinh \Theta_{vb}} \right) \exp(\Theta_{vb} \coth \Theta_{vb} - \Theta_{v2} \coth \Theta_{v2}) \quad (4-72)$$

$$\frac{p_2}{p_1} = \frac{1 + \gamma_1 M_1^2 \sin^2 \beta}{1 + \gamma_2 M_2^2 \sin^2 (\beta - \phi_2)} \quad (4-17)$$

As for the $\delta=0$ case, we use for C_{pb}

$$\delta = 1 \Rightarrow C_{pb} = \frac{2 \left(\frac{p_2}{p_1} P_b - 1 \right)}{\gamma_1 M_1^2}$$

We determine M_b with equation (3-11) and γ_b from subroutine 'thetav'

$$\delta = 1 \Rightarrow M_b = \sqrt{\frac{7}{\gamma_b} \left(\frac{\Theta_{vb}}{\Theta_{v0}} - 1 \right) + \frac{2\Theta_{vb}}{\gamma_b} (\coth \Theta_{v0} - \coth \Theta_{vb})}$$

5.1 VALIDATION

NACA Report 1135 [10] lists $\theta_b - \beta$ tables and diagrams for the plane wedge, weak and strong solution, but only for the perfect gas case. Our results agree with these values to as many digits as they print. Reference values for the Taylor-Maccoll flow perfect gas case are given in reference 11. It only provides the weak solution. Its numbers agree with our values very well. Our computed C_{pb} values compare favorably to the numbers given in reference 11 for the published weak solution.

6. RESULTS

6.1 $\theta_b - \beta$ PLOTS

These plots are depicted on pages 36 and 37. We computed the $\theta_b - \beta$ diagram for the plane wedge for two reasons. First, it allows us to verify the accuracy of the subroutine 'shock' and second, it enables us to point out differences between the flows over a cone and a wedge. In the diagrams, the weak solution is to the left of the θ_b -maximum. Accordingly, the strong solution is to the right of the θ_b -maximum. In practical applications, the shock angle β is usually given by the weak solution. The strong solution, however is of theoretical interest.

The shock is no longer attached to the cone's apex when the semi-vertex angle θ_b becomes larger than the maximum θ_b values of the curves in the diagrams. The diagrams show that the maximum semi-vertex angles θ_b are larger for the cone than for the wedge, especially for small M_1 values. Curves for the imperfect gas model have larger θ_b values than the perfect gas model. Furthermore, this effect increases with increasing stagnation temperature and increasing M_1 .

Curves for the perfect and imperfect gas cases with $\Theta_{v_0} = 5.0$ essentially coincide for the flow over a plane wedge and over a cone. This meets our expectations for the limiting case $T \ll T_v$ and proves the general procedure for the imperfect gas to be correct.

The shock angle β , for a fixed semi-vertex angle θ_b , is smaller for the imperfect gas than computed for the perfect gas, when considering the weak solution. This means that the perfect gas model predicts the shock to be stronger than it actually is. The opposite is true for the strong solution.

The curves for Taylor-Maccoll flow show that a variation of the body angle θ_b between 0° and $\sim 5^\circ$ has, contrary to the flow over a planar wedge, only a very limited effect on the shock angle β . This observation is valid for the weak and also for the strong solution.

It is difficult to give a global estimate for the error of our calculations, but we made the integration step size $\Delta\eta$ so small that a further decrease did not give any change in the calculated digits. We applied the same procedure to the subroutine 'shock' to calculate the β values for the plane oblique shock. We chose the allowed difference between the old and the new values (see page 34) small enough to avoid further change of the computed values. All together, we can say, that the digits shown in tables 1-38 are significant digits.

6.2 $\theta_b - C_{pb}$ PLOT

The reader will find this plot on page 38. It was only necessary to compute the C_{pb} values for the Taylor-Maccoll flow, because the pressure remains constant from behind the shock to the body for the flow over a plane wedge. In this case, C_{pb} may be computed from the shock tables provided in the thesis of M.L.Bultman.²

As with β , we also have a weak and a strong solution. The demarcation between these solutions is at the maximum value of θ_b . The weak solution has lower C_{pb} values than the strong solution. Thus, the weak solution causes far less drag than the strong solution.

C_{pb} increases rapidly with small θ_b , but then slows down with larger θ_b values. For the weak solution, there is virtually no difference between the imperfect and perfect cases, except near detachment. One interesting point is that C_{pb} can be double valued for the strong solution. Sometimes the two θ_b values are for a strong solution, and sometimes one is weak.

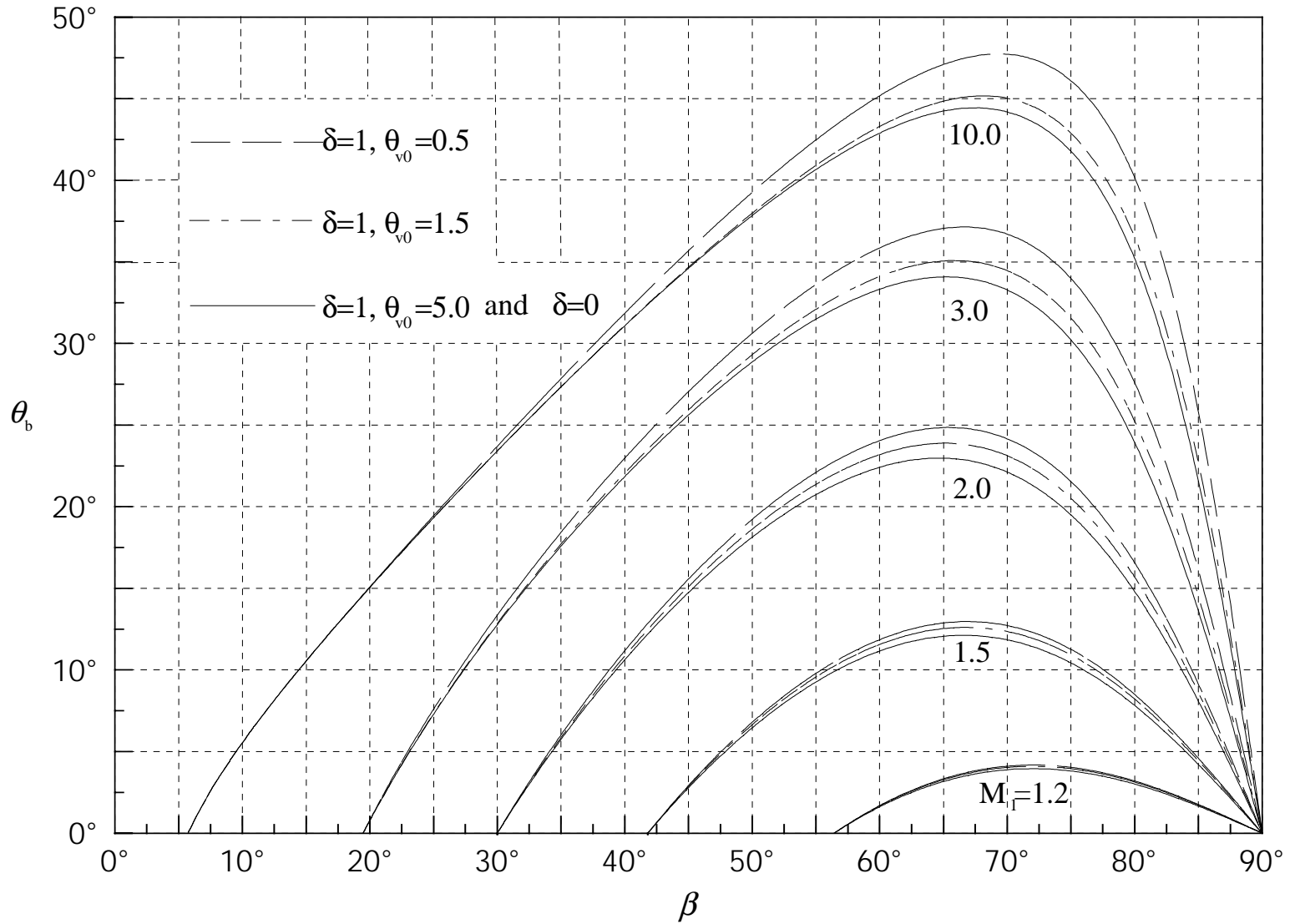


Figure 3 θ_b vs. β for plane oblique shock

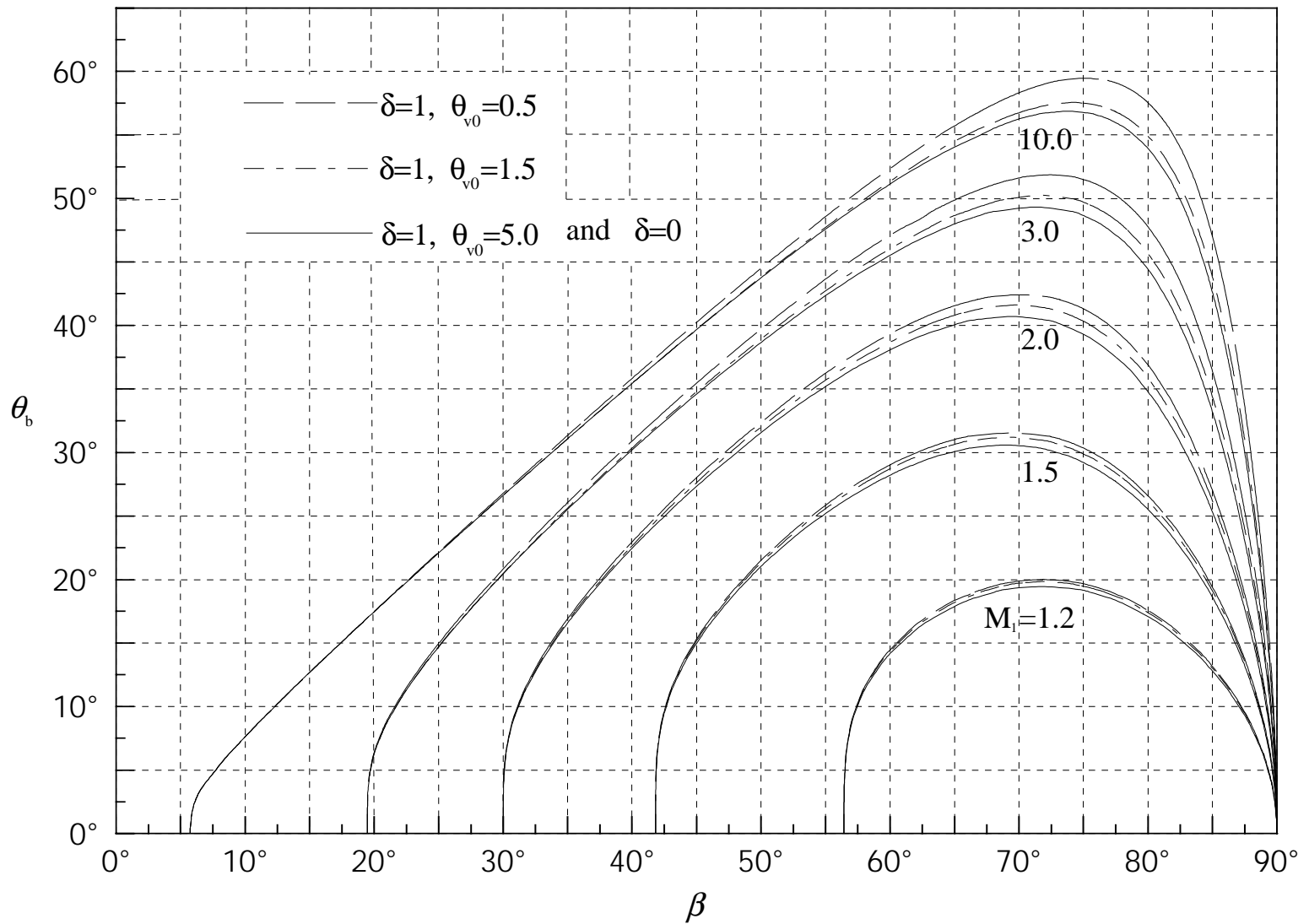


Figure 4 θ_b vs. β for Taylor-Maccoll flow

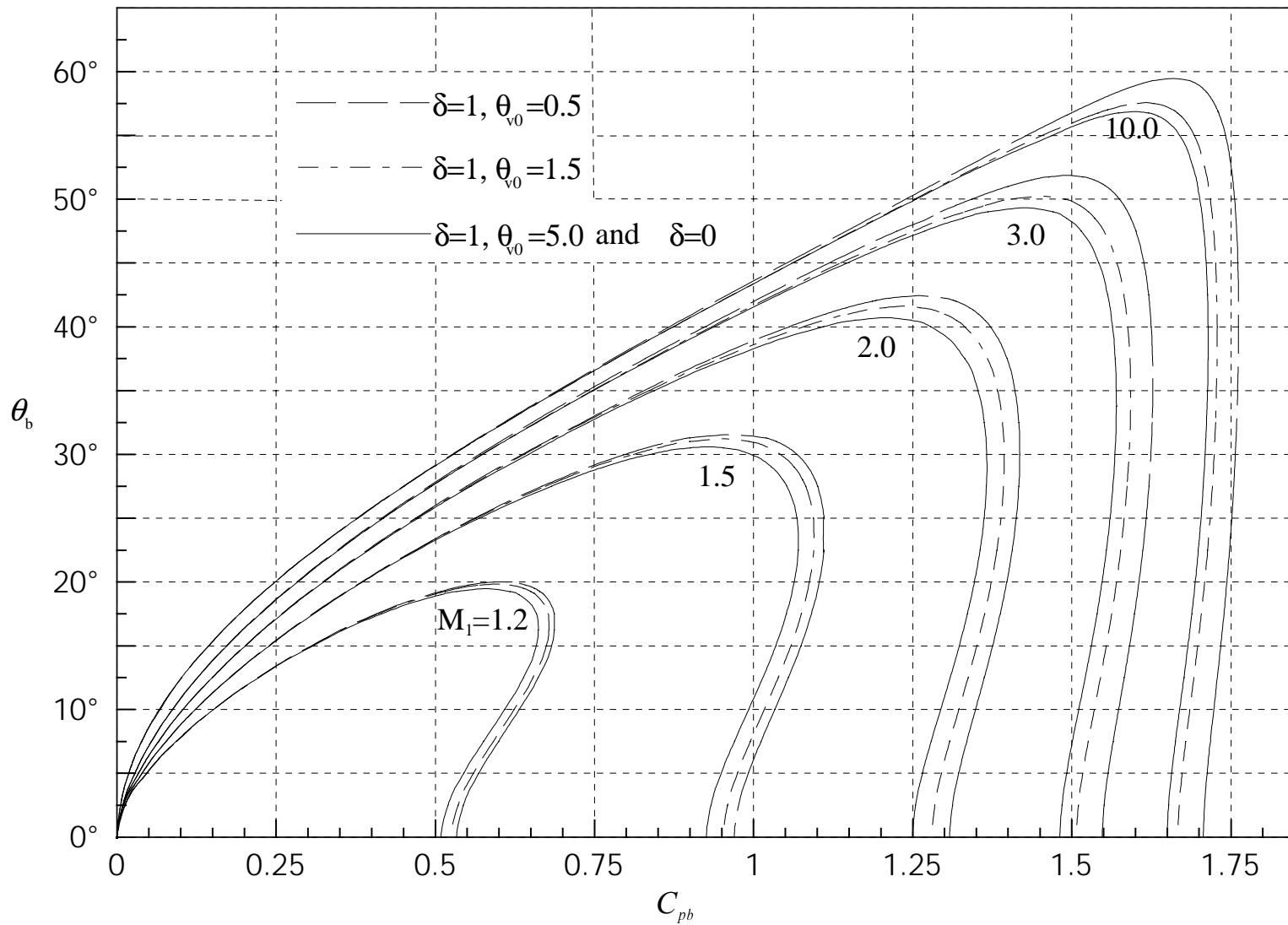


Figure 5 θ_b vs. C_{pb} for Taylor-Maccoll flow

6.3 WEAK SOLUTION COMPARISONS

Our interest is committed to the weak solution, because only this solution occurs in practice. We computed comparisons between imperfect and perfect values for the shock angle β , for the Mach number right behind the shock M_2 , for the Mach number at the body M_b , and for the surface pressure coefficient C_{pb} . We chose the typical semi vertex angle $\theta_b = 10^\circ$. The reader may find the graphs on pages 49-51.

From the diagrams, we observe that the difference between the values computed with the perfect gas model and the values computed with the imperfect gas model does not exceed 2% for any Mach number. Vibrational effects become negligible for Mach numbers M_1 approaching 10. The reason for this is the very large thermal energy associated with the translational and rotational modes in the flow downstream of the shock. All evaluated properties show the same general Mach number trend. The perfect gas model predicts the shock angle β and the surface pressure coefficient C_{pb} generally to be too large, whereas the Mach number right behind the shock M_2 and the Mach number at the body M_b are generally predicted to be too small by the perfect gas model.

The diagrams also point out that vibrational effects increase with increasing temperature, as expected. All the evaluated properties have a local extremum at low supersonic Mach numbers. The lowest possible Mach number for a semi-vertex angle $\theta_b = 10^\circ$ is about 1.06 (see figures 6-9). For a lower Mach number, the shock detaches. The

near vertical behaviour of the curves in all four figures, when $M_1 - 1$ is small, is caused by the perfect solution detaching at a θ_b value while the imperfect solution is still attached. The same phenomenon occurs in the strong solution comparison.

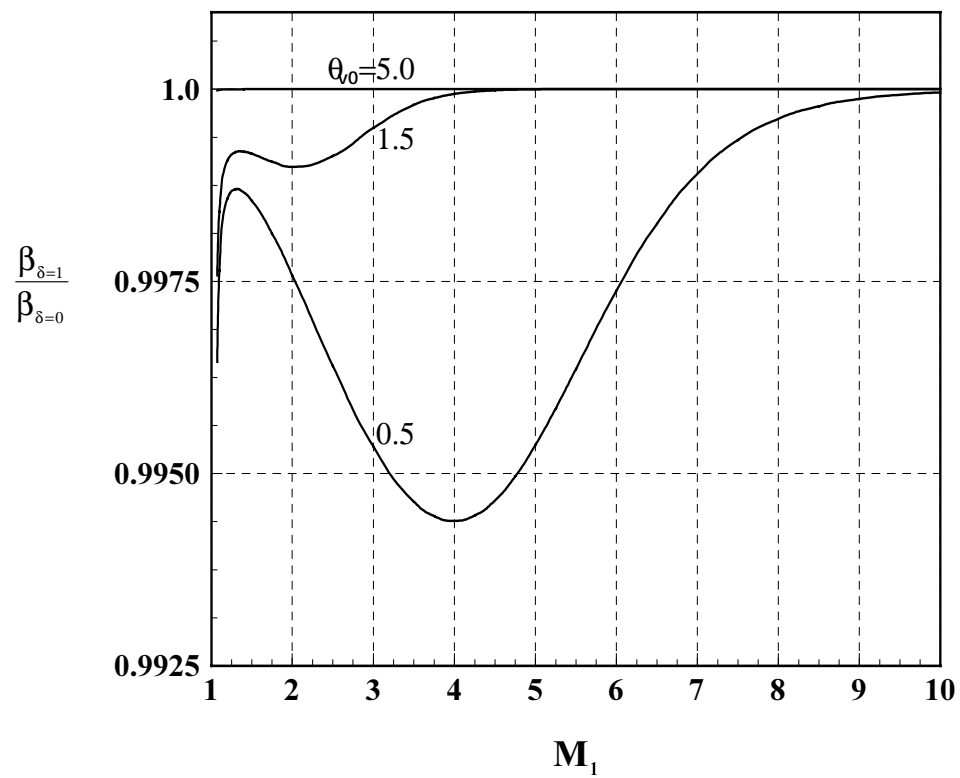


Figure 6 β comparison; $\theta_b=10^\circ$; weak solution

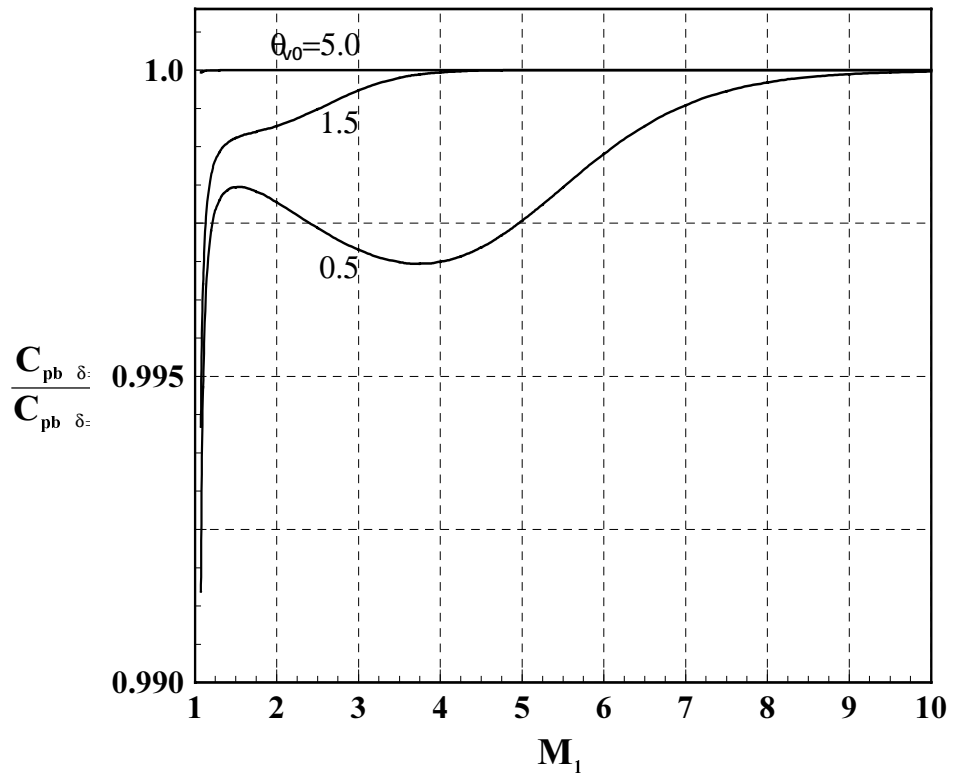


Figure 7 C_{pb} comparison; $\theta_b=10^\circ$; weak solution

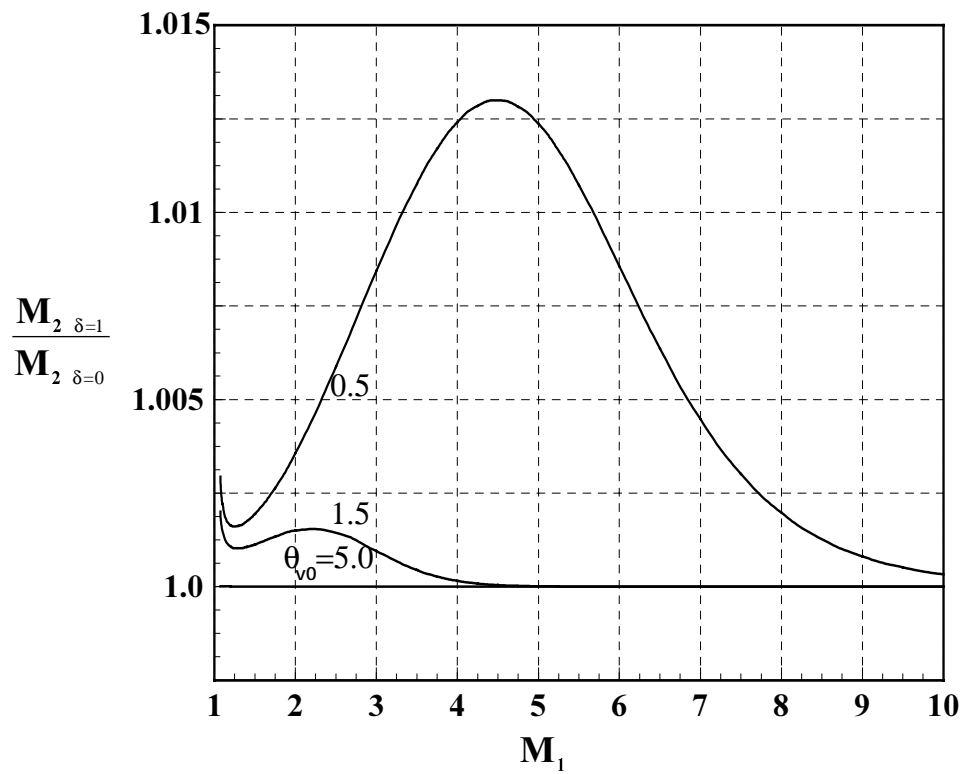


Figure 8 M_2 comparison; $\theta_b=10^\circ$; weak solution

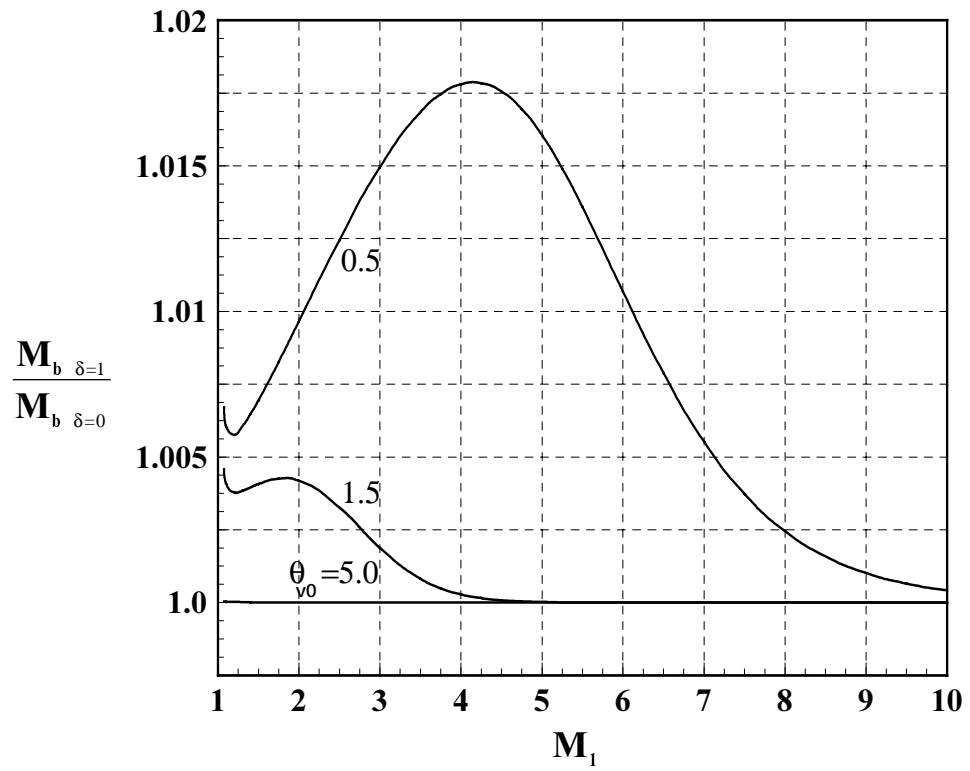


Figure 9 M_b comparison; $\theta_b=10^\circ$; weak solution

6.4 STRONG SOLUTION COMPARISONS

As mentioned earlier, the strong solution is only of theoretical interest. The reader may find the diagrams on pages 52-54. For the strong solution, the perfect gas model predicts the properties to be up to 6% different from the imperfect gas model. As expected, the values differ more for higher temperatures. For $\Theta_{v_0} = 5.0$, both gas models are essentially identical. The difference between perfect and imperfect values does not disappear for higher Mach numbers.

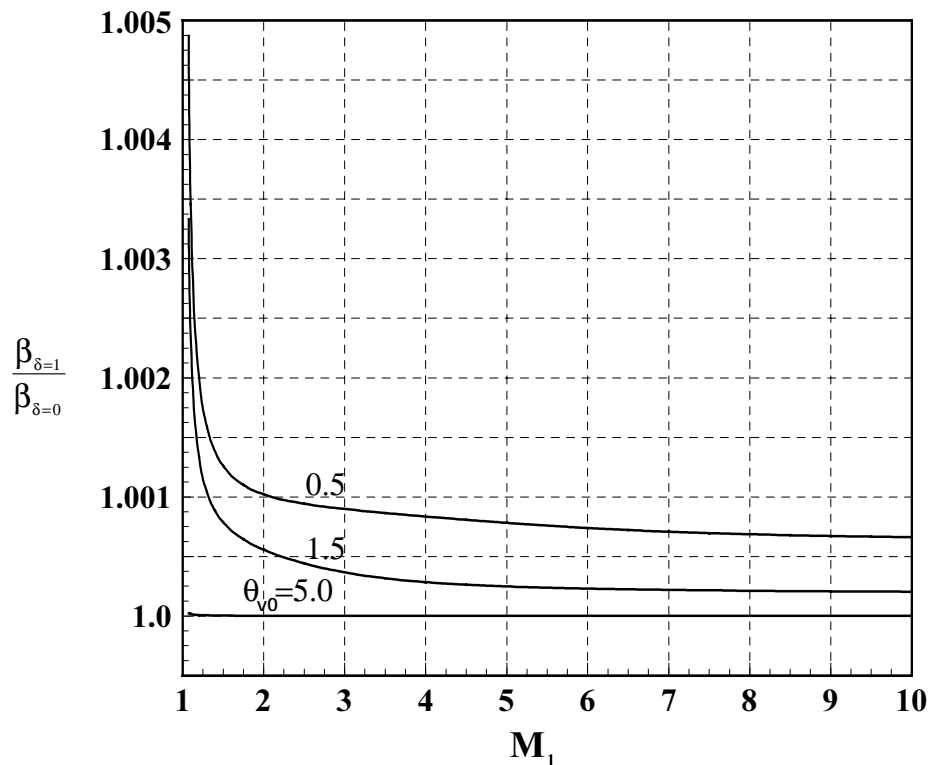


Figure 10 β comparison; $\theta_b = 10^\circ$; strong solution

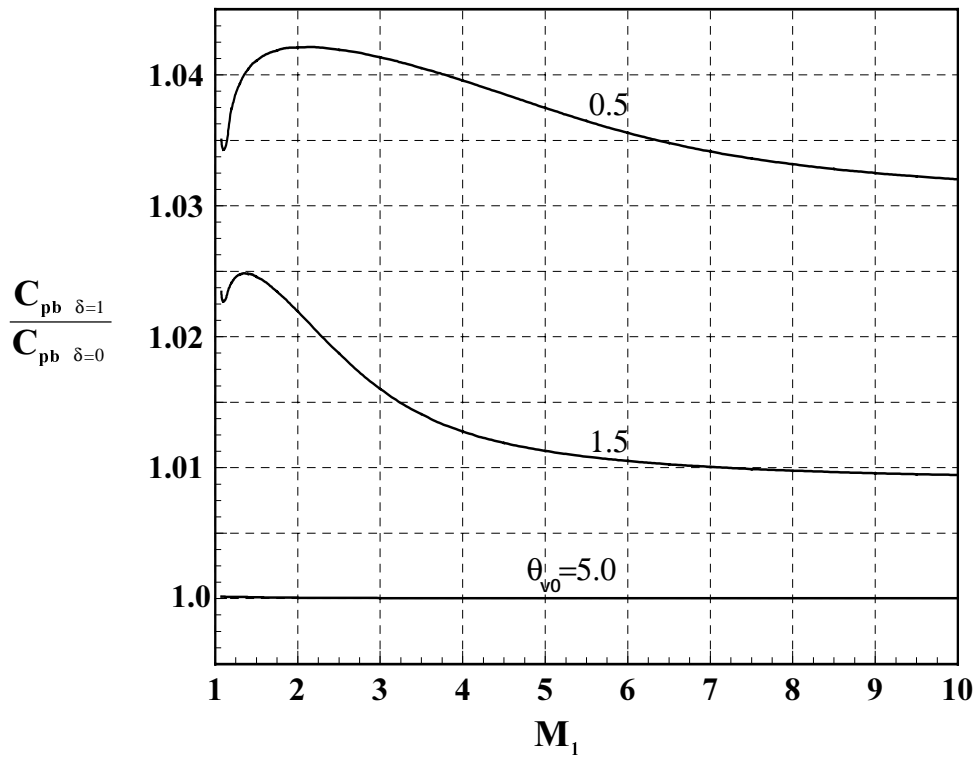


Figure 11 C_{pb} comparison; $\theta_b=10^\circ$; strong solution

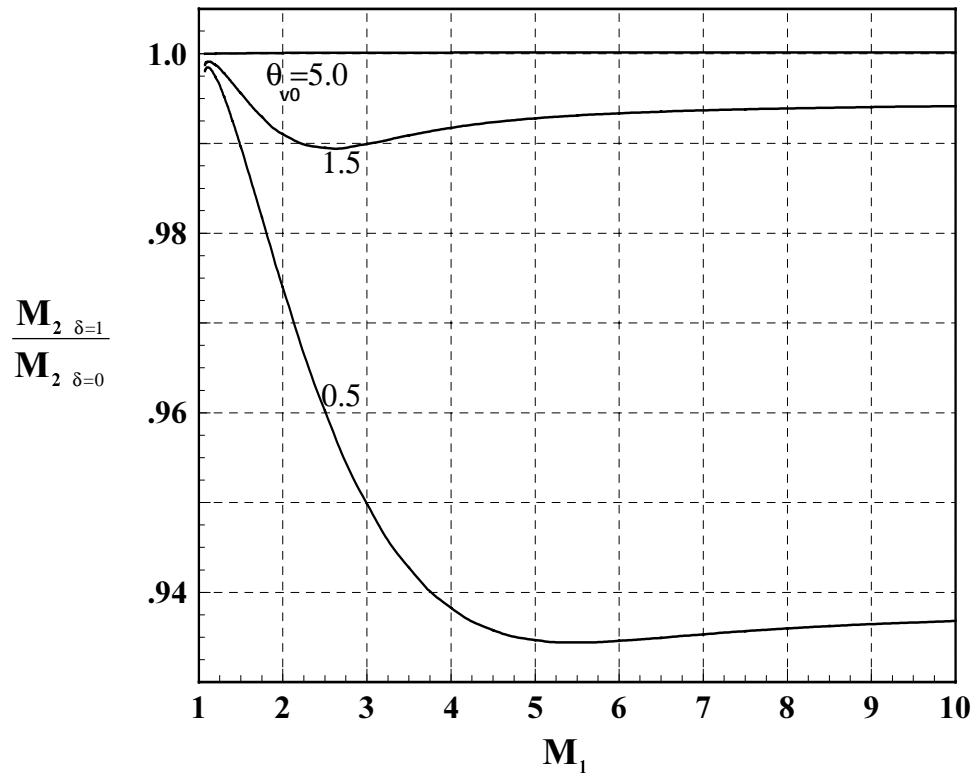


Figure 12 M_2 comparison; $\theta_b=10^\circ$; strong solution

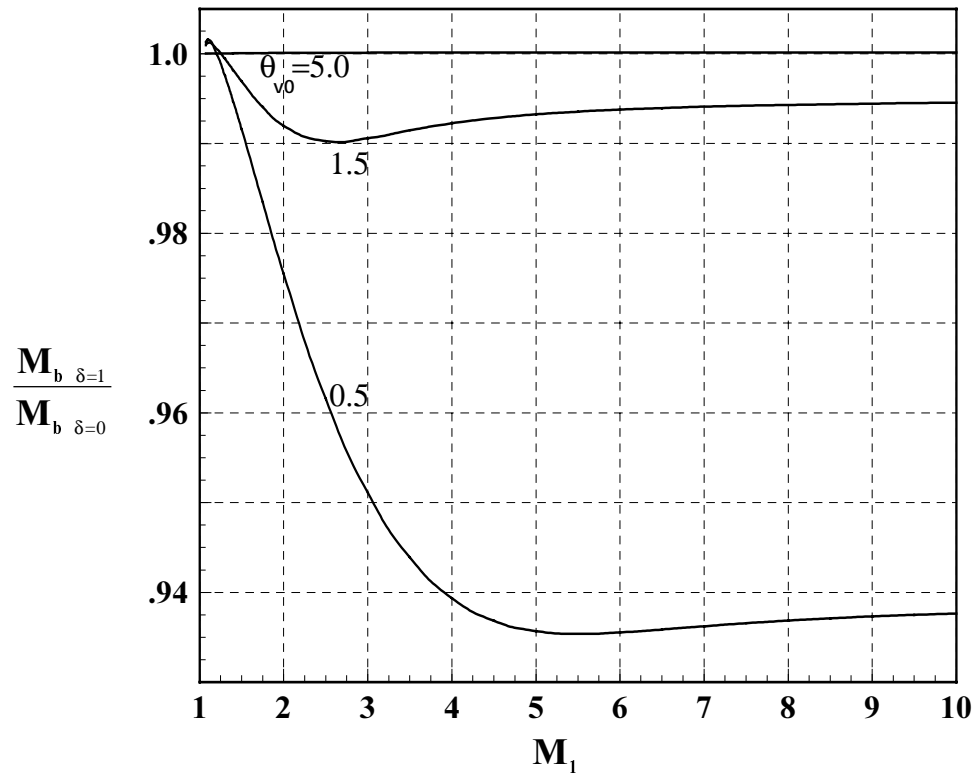


Figure 12 M_b comparison; $\theta_b=10^\circ$; strong solution

REFERENCES

1. Christy, G.J., *Calorically Imperfect Isentropic Flow*, M.S.Thesis, University of Oklahoma, Norman, 1993.
2. Bultman, M.L., *Thermally Perfect, Calorically Imperfect Planar Shock Flow*, M.S.Thesis, University of Oklahoma, Norman, 1994.
3. Ismail, M., *Prandtl-Meyer Flow of a Calorically Imperfect Gas*, M.S.Thesis, University of Oklahoma, Norman, 1994.
4. Vincenti, W.G. and Kruger, C.H.Jr., *Introduction to Physical Gas Dynamics*, John Wiley, New York, 1986.
5. Emanuel, G., *Advanced Classical Thermodynamics*, AIAA Education Series, Washington, D.C., 1987.
6. Emanuel, G., *Analytical Fluid Dynamics*, CRC Press, Boca Raton, 1994.
7. Landau, L.D. and Lifshitz, E.M., *Fluid Mechanics*, Pergamon Press, New York, 1987.

8. Kincaid, D. and Cheney, W., *Numerical Analysis*, Brooks/Cole Publishing Company, Pacific Grove, 1990.
9. Engeln-Müllges, G., *Angewandte Mathematik*, FH Aachen, Aachen, 1991.
10. Ames Research Staff, *Equations, Tables, and Charts for Compressible Flow*, NACA Report 1135, 1953.
11. Sims, J.L., *Tables for Supersonic Flow around Right Circular Cones at Zero Angle of Attack*, U.S. Government Printing Office, Washington, D.C., 1964.

θ_b	β			
	perfect gas	imperfect gas		
		Θ_{v0}		
		5.0	1.5	0.5
0.00	56.44269	56.44269	56.44269	56.44269
0.50	57.45735	57.45722	57.42620	57.40918
1.00	58.54787	58.54759	58.47969	58.44258
1.50	59.73481	59.73433	59.62117	59.55962
2.00	61.05010	61.04935	60.87798	60.78544
2.50	62.54837	62.54723	62.29546	62.16102
3.00	64.33903	64.33725	63.95949	63.76187
3.50	66.72020	66.71695	66.07798	65.76113
3.60	67.34450	67.34063	66.60174	66.24409
3.70	68.06960	68.06478	67.18285	66.77173
3.80	68.96865	68.96204	67.84551	67.35931
3.90	70.30605	70.29335	68.63791	68.03341
4.00			69.69033	68.84895
4.10				69.96794

Table 1 β vs. θ_b for plane oblique shock; $M_1=1.2$; weak solution

θ_b	β			
	perfect gas	imperfect gas		
		Θ_{v0}		
		5.0	1.5	0.5
0.00	90.00000	90.00000	90.00000	90.00000
0.50	88.53242	88.53275	88.59097	88.62209
1.00	87.04050	87.04117	87.16017	87.22371
1.50	85.49602	85.49707	85.68263	85.78153
2.00	83.86116	83.86264	84.12559	84.26524
2.50	82.07657	82.07860	82.43939	82.62976
3.00	80.02911	80.03193	80.53467	80.79621
3.50	77.41753	77.42197	78.20063	78.58870
3.60	76.75008	76.75516	77.63656	78.06681
3.70	75.98277	75.98883	77.01602	77.50111
3.80	75.04242	75.05030	76.31482	76.87632
3.90	73.66462	73.67862	75.48473	76.16585
4.00			74.39546	75.31475
4.10				74.16101

Table 2 β vs. θ_b for plane oblique shock; $M_1=1.2$; strong solution

θ_b	β			
	perfect gas	imperfect gas		
		Θ_{v0}		
		5.0	1.5	0.5
0.00	41.81031	41.81031	41.81031	41.81031
2.50	44.66076	44.66064	41.58003	44.52033
5.00	47.88926	47.88895	47.69468	47.55348
7.50	51.70250	51.70180	51.32723	51.06311
10.00	56.67868	56.67694	55.92132	55.42182
11.00	59.46511	59.46215	58.33347	57.63688
11.50	61.33632	61.33182	59.81101	58.94420
11.60	61.79144	61.78639	60.14232	59.22962
11.70	62.29191	62.28611	60.48967	59.52507
11.80	62.85561	62.84874	60.85583	59.83176
11.90	63.51665	63.50804	61.24445	60.15119
12.00	64.35881	64.34650	61.66052	60.48521
12.10	65.84456	65.80633	62.11123	60.83617
12.20			62.60758	61.20714
12.30			63.16805	61.60223
12.40			63.82836	62.02720
12.50			64.67948	62.49052
12.60			66.38418	63.00567
12.70				63.59648
12.80				64.31382

Table 3 β vs. θ_b for plane oblique shock; $M_1=1.5$; weak solution

θ_b	β			
	perfect gas	imperfect gas		
		Θ_{v0}		
		5.0	1.5	0.5
0.00	90.00000	90.00000	90.00000	90.00000
2.50	87.07526	87.07585	87.22596	87.32301
5.00	83.98938	83.99063	84.31038	84.51662
7.50	80.49750	80.49958	81.04561	81.39528
10.00	75.99487	75.99843	76.96362	77.56353
11.00	73.43591	73.44088	74.79251	75.59410
11.50	71.68605	71.69265	73.44272	74.41661
11.60	71.25579	71.26296	73.13754	74.15769
11.70	70.78039	70.78832	72.81649	73.88893
11.80	70.24194	70.25095	72.47681	73.60911
11.90	69.60634	69.61712	72.11487	73.31673
12.00	68.78982	68.80431	71.72566	73.00993
12.10	67.32991	67.37034	71.30199	72.68637
12.20			70.83286	72.34298
12.30			70.29980	71.97564
12.40			69.66707	71.57860
12.50			68.84371	71.14337
12.60			67.16696	70.65650
12.70				70.09413
12.80				69.40541

Table 4 β vs. θ_b for plane oblique shock; $M_1=1.5$; strong solution

θ_b	β			
	perfect gas	imperfect gas		
		Θ_{v0}		
		5.0	1.5	0.5
0.00	30.00000	30.00000	30.00000	30.00000
2.50	32.07280	32.07280	32.03316	31.97662
5.00	34.30157	34.30156	34.21281	34.08950
7.50	36.70593	36.70591	36.55563	36.35317
10.00	39.31393	39.31388	39.08506	38.78764
12.00	41.57519	41.57511	41.26612	40.87750
12.50	42.16881	42.16871	41.83648	41.42235
15.00	45.34362	45.34343	44.86783	44.30387
17.50	48.97951	48.97914	48.28526	47.51339
20.00	53.42294	53.42210	52.32336	51.21528
22.50	60.39841	60.39437	57.77274	55.85448
22.60	60.89015	60.88542	58.05846	56.07582
22.70	61.44905	61.44329	58.35431	56.30142
22.80	62.11746	62.10987	58.66160	56.53159
22.90	63.01965	63.00727	58.98196	56.76665
23.00			59.31747	57.00700
23.50			61.36017	58.30571
23.60			61.90345	58.58967
23.70			62.55017	58.88393
23.80			63.41220	59.18989
24.00				59.84425
24.50				61.90459

Table 5 β vs. θ_b for plane oblique shock; $M_1=2.0$; weak solution

θ_b	β			
	perfect gas	imperfect gas		
		Θ_{v0}		
		5.0	1.5	0.5
0.00	90.00000	90.00000	90.00000	90.00000
2.50	88.49571	88.49597	88.59064	88.67437
5.00	86.96511	86.96563	87.15813	87.32833
7.50	85.37880	85.37959	85.67678	85.93943
10.00	83.70008	83.70116	84.11509	84.48052
12.00	82.25702	82.25836	82.77970	83.23924
12.50	81.87785	81.87926	82.43021	82.91557
15.00	79.83169	79.83348	80.55718	81.19176
17.50	77.41348	77.41578	78.38311	79.22193
20.00	74.27014	74.27325	75.66698	76.83594
22.50	68.67082	68.67751	71.61202	73.58334
22.60	68.23562	68.24301	71.38350	73.41886
22.70	67.73337	67.74181	71.14495	73.25023
22.80	67.12174	67.13201	70.89508	73.07713
22.90	66.27642	66.29150	70.63223	72.89923
23.00			70.35434	72.71616
23.50			68.60132	71.70535
23.60			68.11628	71.47929
23.70			67.52791	71.24301
23.80			66.72433	70.99514
24.00				70.45726
24.50				68.68985

Table 6 β vs. θ_b for plane oblique shock; $M_1=2.0$; strong solution

θ_b	β			
	perfect gas	imperfect gas		
		Θ_{v0}		
		5.0	1.5	0.5
0.00	19.47122	19.47122	19.47122	19.47122
2.50	21.22996	21.22996	21.22253	21.15671
5.00	23.13326	23.13326	23.11575	22.97280
7.50	25.18350	25.18350	25.15242	24.92047
10.00	27.38269	27.38269	27.33337	27.00004
12.50	29.73345	29.73345	29.65970	29.21185
15.00	32.24040	32.24040	32.13391	31.55718
17.50	34.91204	34.91203	34.76161	34.03941
20.00	37.76363	37.76363	37.55381	36.66558
22.50	40.82215	40.82214	40.53077	39.44871
25.00	44.13593	44.13591	43.72908	42.41174
27.50	47.79763	47.79757	47.21710	45.59524
30.00	52.01384	52.01366	51.13680	49.07481
32.50	57.45367	57.45295	55.86601	53.01086
33.00	58.90888	58.90781	56.99983	53.88144
33.50	60.70471	60.70284	58.24983	54.79133
34.00	63.67317	63.66577	59.67854	55.74899
34.50			61.43870	56.76647
35.00			64.33613	57.86197
35.50				59.06536
36.00				60.43238

Table 7 β vs. θ_b for plane oblique shock; $M_1 = 3.0$; weak solution

θ_b	β			
	perfect gas	imperfect gas		
		Θ_{v0}		
		5.0	1.5	0.5
0.00	90.00000	90.00000	90.00000	90.00000
2.50	89.12362	89.12376	89.18135	89.26880
5.00	88.23890	88.23917	88.35521	88.53143
7.50	87.33703	87.33743	87.51372	87.78146
10.00	86.40825	86.40879	86.64819	87.01182
12.50	85.44114	85.44182	85.74855	86.21447
15.00	84.42168	84.42252	84.80256	85.37980
17.50	83.33177	83.33276	83.79462	84.49589
20.00	82.14667	82.14784	82.70382	83.54721
22.50	80.83041	80.83177	81.50040	82.51259
25.00	79.32621	79.32780	80.13899	81.36145
27.50	77.53372	77.53559	78.54317	80.04620
30.00	75.23939	75.24165	76.56382	78.48486
32.50	71.76789	71.77102	73.81678	76.51127
33.00	70.71142	70.71498	73.08391	76.03804
33.50	69.31593	69.32036	72.23628	75.52701
34.00	66.74936	66.75939	71.21131	74.96970
34.50			69.85622	74.35403
35.00			67.36517	73.66176
35.50				72.86299
36.00				71.90193

Table 8 β vs. θ_b for plane oblique shock; $M_1=3.0$; strong solution

θ_b	β			
	perfect gas	imperfect gas		
		Θ_{v0}		
		5.0	1.5	0.5
0.00	5.73917	5.73917	5.73917	5.73917
2.50	7.45009	7.45009	7.45009	7.45008
5.00	9.51931	9.51931	9.51931	9.51922
7.50	11.87061	11.87061	11.87061	11.87003
10.00	14.42659	14.42659	14.42659	14.42337
12.50	17.12936	17.12936	17.12936	17.11630
15.00	19.94158	19.94158	19.94158	19.90249
17.50	22.84141	22.84141	22.84141	22.75045
20.00	25.81779	25.81779	25.81772	25.64296
22.50	28.86737	28.86737	28.86688	28.57461
25.00	31.99312	31.99312	31.99083	31.54800
27.50	35.20417	35.20417	35.19621	34.57093
30.00	38.51714	38.51714	38.49506	37.65546
32.50	41.95943	41.95943	41.90774	40.81863
35.00	45.57687	45.57687	45.46952	44.08512
37.50	49.45198	49.45197	49.24491	47.49287
40.00	53.75818	53.75816	53.36538	51.10596
42.30	58.51939	58.51924	57.74441	54.71653
43.00	60.31387	60.31357	59.29700	55.89834
43.50	61.82106	61.82055	60.52162	56.77539
44.00	63.73544	63.73432	61.89851	57.68582
44.50			63.54753	58.63694
45.00			65.95957	59.63908
45.50				60.70760
46.00				61.86726
46.50				63.16280
47.00				64.69310
47.50				66.80798

Table 9 β vs. θ_b for plane oblique shock; $M_1=10.0$; weak solution

θ_b	β			
	perfect gas	imperfect gas		
		Θ_{v0}		
		5.0	1.5	0.5
0.00	90.00000	90.00000	90.00000	90.00000
2.50	89.46911	89.46919	89.49950	89.56998
5.00	88.93469	88.93484	88.99575	89.13735
7.50	88.39309	88.39332	88.48535	88.69940
10.00	87.84042	87.84072	87.96474	88.25329
12.50	87.27236	87.27275	87.42994	87.79589
15.00	86.68404	86.68451	86.87650	87.32371
17.50	86.06974	86.07028	86.29917	86.83273
20.00	85.42252	85.42316	85.69169	86.31820
22.50	84.73379	84.73451	85.04629	85.77435
25.00	83.99245	83.99327	84.35304	85.19401
27.50	83.18371	83.18464	83.59883	84.56795
30.00	82.28695	82.28799	82.76560	83.88392
32.50	81.27180	81.27297	81.82717	83.12500
35.00	80.09027	80.09158	80.74310	82.26669
37.50	78.65816	78.65965	79.44483	81.27109
40.00	76.80079	76.80251	77.79819	80.07404
42.30	74.29680	74.29889	75.69090	78.68956
43.00	73.19001	73.19233	74.82883	78.18587
43.50	72.17421	72.17682	74.09718	77.79336
44.00	70.75138	70.75467	73.21305	77.36761
44.50			72.05658	76.90130
45.00			70.13687	76.38411
45.50				75.80067
46.00				75.12623
46.50				74.31604
47.00				73.27121
47.50				71.64194

Table 10 β vs. θ_b for plane oblique shock; $M_1=10.0$; strong solution

θ_b	β			
	perfect gas	imperfect gas		
		Θ_{v_0}		
		5.0	1.5	0.5
0.00	56.44269	56.44269	56.44269	56.44269
2.50	56.44552	56.44552	56.44521	56.44504
5.00	56.51392	56.51390	56.50983	56.50920
7.50	56.79288	56.79280	56.77782	56.76682
10.00	57.48242	57.48219	57.42917	57.40079
12.50	58.76590	58.76515	58.64939	58.58640
15.00	60.87422	60.87198	60.64924	60.52787
17.50	64.30709	64.25993	63.80286	63.54507
19.00	68.09605	68.05084	67.03021	66.57071
19.25	69.22639	69.24944	67.84714	67.29247
19.50			68.80819	68.09603
19.75			70.48872	69.22126
20.00				71.63678

Table 11 β vs. θ_b for Taylor-Maccoll flow; $M_1=1.2$; weak solution

θ_b	β			
	perfect gas	imperfect gas		
		Θ_{v0}		
		5.0	1.5	0.5
0.00	90.00000	90.00000	90.00000	90.00000
2.50	89.82994	89.82998	89.83591	89.83886
5.00	89.30146	89.30161	89.32472	89.33629
7.50	88.38500	88.38534	88.44644	88.48195
10.00	87.06303	87.06379	87.17997	87.23820
12.50	85.23791	85.23880	85.42697	85.52960
15.00	82.80097	82.80227	83.10871	83.27240
17.50	79.24213	79.24403	79.81676	80.10015
19.00	75.50256	75.52402	76.65081	77.16111
19.25	74.31968	74.32687	75.84319	76.44502
19.50			74.84041	75.62259
19.75			73.24184	74.53509
20.00				72.15767

Table 12 β vs. θ_b for Taylor-Maccoll flow; $M_1=1.2$; strong solution

θ_b	β			
	perfect gas	imperfect gas		
		Θ_{v0}		
		5.0	1.5	0.5
0.00	41.81031	41.81031	41.81031	41.81031
2.50	41.81402	41.81201	41.81178	41.81161
5.00	41.87071	41.87005	41.86707	41.86491
7.50	42.10654	42.10652	42.09204	42.08150
10.00	42.65976	42.65971	42.62391	42.59778
12.50	43.62524	43.62511	43.55700	43.50216
15.00	45.02336	45.02309	44.90082	44.81982
17.50	46.83015	46.82965	46.65177	46.52185
20.00	49.01133	49.01042	48.76213	48.61556
22.50	51.61502	51.61332	51.25908	51.04943
25.00	54.75303	54.74925	54.24169	53.93270
27.50	58.66098	58.63933	57.86897	57.37846
28.00	59.59874	59.59896	58.74501	58.22053
29.00	61.75539	61.77161	60.56109	59.95754
30.00	64.76673	64.75091	63.01373	62.09982
30.50	67.61222	67.59622	64.53310	63.37443
31.00			66.77684	64.94855
31.25				65.96620
31.30				66.21489

Table 13 β vs. θ_b for Taylor-Maccoll flow; $M_1=1.5$; weak solution

θ_b	β			
	perfect gas	imperfect gas		
		Θ_{v0}		
		5.0	1.5	0.5
0.00	90.00000	90.00000	90.00000	90.00000
2.50	89.91057	89.91059	89.91464	89.91706
5.00	89.64181	89.64189	89.65769	89.66719
7.50	89.18892	89.18909	89.22942	89.25044
10.00	88.56294	88.56328	88.61997	88.66039
12.50	87.75256	87.75300	87.86307	87.92808
15.00	86.76255	86.76317	86.92508	87.01580
17.50	85.58623	85.58706	85.81086	85.94279
20.00	84.19318	84.19425	84.49249	84.67453
22.50	82.52783	82.52919	82.93410	83.19200
25.00	80.49015	80.49186	81.05366	81.39369
27.50	77.77301	77.77519	78.61342	79.09266
28.00	77.06561	77.06793	77.99548	78.53614
29.00	75.40203	75.41872	76.59612	77.26153
30.00	72.93210	72.93888	74.75126	75.66795
30.50	70.34448	70.35799	73.48655	74.65562
31.00			71.50705	73.34574
31.25				72.46504
31.30				72.24794

Table 14 β vs. θ_b for Taylor-Maccoll flow; $M_1=1.5$; strong solution

θ_b	β			
	perfect gas	imperfect gas		
		Θ_{v0}		
		5.0	1.5	0.5
0.00	30.00000	30.00000	30.00000	30.00000
2.50	30.00403	30.00403	30.00380	30.00348
5.00	30.09449	30.09448	30.09127	30.08671
7.50	30.44365	30.44364	30.42905	30.41500
10.00	31.19382	31.19381	31.16235	31.11835
12.50	32.38155	32.38154	32.32716	32.24306
15.00	33.91031	33.91029	33.81843	33.70334
17.50	35.72017	35.72013	35.58631	35.43851
20.00	37.77828	37.77821	37.62820	37.41673
22.50	40.04448	40.04437	39.85892	39.57991
25.00	42.53175	42.53156	42.23715	41.95012
27.50	45.18664	45.18631	44.85998	44.44432
30.00	48.12539	48.04810	47.60399	47.19148
32.50	51.21289	51.21173	50.64988	50.17415
35.00	54.74470	54.74398	54.02877	53.32315
37.50	58.89971	58.89787	57.87911	56.92332
40.00	64.86472	64.85708	62.81654	61.29108
40.50	67.09223	67.09655	64.11251	62.34801
41.00			65.72400	63.51528
41.50			68.37622	64.87111
42.00				66.58925
42.10				67.02864
42.25				67.79850

Table 15 β vs. θ_b for Taylor-Maccoll flow; $M_1=2.0$; weak solution

θ_b	β			
	perfect gas	imperfect gas		
		Θ_{v0}		
		5.0	1.5	0.5
0.00	90.00000	90.00000	90.00000	90.00000
2.50	89.94761	89.94762	89.95064	89.95314
5.00	89.78844	89.78848	89.80265	89.81255
7.50	89.52840	89.52849	89.55804	89.58002
10.00	89.16955	89.16972	89.21924	89.26072
12.50	88.72052	88.72075	88.79580	88.85979
15.00	88.18056	88.18089	88.29125	88.38064
17.50	87.55079	87.55122	87.70300	87.82797
20.00	86.83738	86.83792	87.02990	87.19615
22.50	86.02950	86.03017	86.28346	86.48893
25.00	85.12691	85.12772	85.43405	85.70116
27.50	84.09605	84.09702	84.48446	84.81411
30.00	82.91962	82.92077	83.40513	83.80889
32.50	81.52991	81.53127	82.13720	82.64460
35.00	79.82826	79.82988	80.61264	81.25547
37.50	77.52697	77.52893	78.61970	79.51104
40.00	73.45145	73.47062	75.57913	77.02758
40.50	71.59123	71.60264	74.65169	76.35071
41.00			73.42209	75.56388
41.50			71.17026	74.59685
42.00				73.26296
42.10				72.90454
42.25				72.24034

Table 16 β vs. θ_b for Taylor-Maccoll flow; $M_1=2.0$; strong solution

θ_b	β			
	perfect gas	imperfect gas		
		Θ_{v0}		
		5.0	1.5	0.5
0.00	19.47122	19.47122	19.47122	19.47122
2.50	19.48689	19.48689	19.48677	19.48570
5.00	19.71510	19.71510	19.71355	19.69946
7.50	20.44950	20.44950	20.44950	20.39890
10.00	21.71381	21.71381	21.70286	21.61284
12.50	23.35175	23.35175	23.32796	23.18863
15.00	25.25401	25.25401	25.21582	25.03324
17.50	27.35024	27.35024	27.31845	27.06839
20.00	29.60503	29.60503	29.55749	29.26329
22.50	31.98287	31.98287	31.92521	31.55899
25.00	34.47989	34.47989	34.37239	33.96628
27.50	37.07535	37.07534	36.95344	36.46634
30.00	39.77294	39.77226	39.60615	39.05290
32.50	42.58835	42.58833	42.40273	41.72379
35.00	45.48733	45.48728	45.25585	44.48366
37.50	48.55539	48.55528	48.23835	47.35943
40.00	51.77992	51.77408	51.36496	50.36822
42.50	55.24511	55.24440	54.70553	53.52667
45.00	59.13019	59.13111	58.33535	56.86691
47.50	63.89133	63.91102	62.65876	60.68236
48.50	66.48913	66.50218	64.63274	62.54008
49.00	68.34253	68.33564	65.97230	63.28942
49.50			67.39755	64.25637
50.00			69.37519	65.29616
50.50				66.45185
51.00				67.78638
51.25				68.57516
51.50				69.51499
51.75				70.86703

Table 17 β vs. θ_b for Taylor-Maccoll flow; $M_1= 3.0$; weak solution

θ_b	β			
	perfect gas	imperfect gas		
		Θ_{v0}		
		5.0	1.5	0.5
0.00	90.00000	90.00000	90.00000	90.00000
2.50	89.96686	89.96687	89.96893	89.97191
5.00	89.86785	89.86787	89.87601	89.88845
7.50	89.70613	89.70618	89.72513	89.75212
10.00	89.48549	89.48558	89.51830	89.56587
12.50	89.20972	89.20985	89.26059	89.33464
15.00	88.88408	88.88426	88.95479	89.05991
17.50	88.50757	88.50781	88.60303	88.74396
20.00	88.08554	88.08585	88.20884	88.39202
22.50	87.61865	87.61902	87.77287	88.00103
25.00	87.10028	87.10072	87.29169	87.57223
27.50	86.53213	86.53266	86.76209	87.10107
30.00	85.90557	85.90619	86.18179	86.58598
32.50	85.20771	85.20842	85.53670	86.01810
35.00	84.42790	84.42872	84.81398	85.38463
37.50	83.53224	83.53318	83.99919	84.67464
40.00	82.48977	82.49085	83.04678	83.86396
42.50	81.21370	81.21495	81.90657	82.90599
45.00	79.54550	79.55503	80.45769	81.73588
47.50	77.02151	77.02329	78.40596	80.19935
48.50	75.31242	75.32939	77.22325	79.40390
49.00	73.93163	73.93381	76.45415	78.94496
49.50			75.47393	78.43111
50.00			73.94680	77.83945
50.50				77.13977
51.00				76.25712
51.25				75.69068
51.50				74.97140
51.75				73.85151

Table 18 β vs. θ_b for Taylor-Maccoll flow; $M_1=3.0$; strong solution

θ_b	β			
	perfect gas	imperfect gas		
		Θ_{v0}		
		5.0	1.5	0.5
0.00	5.73917	5.73917	5.73917	5.73917
2.50	6.10744	6.10744	6.10744	6.10744
5.00	7.72357	7.72357	7.72357	7.72355
7.50	9.89567	9.89567	9.89567	9.89551
10.00	12.30243	12.30243	12.30243	12.30192
12.50	14.81371	14.81371	14.81371	14.80887
15.00	17.41951	17.41951	17.41951	17.40232
17.50	20.04712	20.04712	20.04712	20.02477
20.00	22.73985	22.73985	22.73984	22.67399
22.50	25.45379	25.45379	25.45372	25.36582
25.00	28.20936	28.20936	28.20896	28.06078
27.50	30.97972	30.97972	30.97802	30.79302
30.00	33.78148	33.78148	33.78243	33.52391
32.50	36.62689	36.62689	36.62707	36.28236
35.00	39.50040	39.50040	39.49822	39.06724
37.50	42.42718	42.42718	42.39916	41.88244
40.00	45.38991	45.38990	45.35661	44.71605
42.50	48.45547	48.45546	48.38838	47.62701
45.00	51.61100	51.61098	51.49608	50.61384
47.50	54.90214	54.90209	54.71751	53.68974
50.00	58.37434	58.37414	58.10632	56.84672
52.50	62.20978	62.21307	61.76352	60.20367
55.00	67.01926	66.79959	65.95863	63.86080
56.00	69.26711	69.26677	68.12897	65.49547
56.50	70.95728	70.95969	69.31429	66.34974
56.75	72.26452	72.25867	70.01326	66.81385
57.00			70.80799	67.25583
57.50			73.39859	68.22491
58.00				69.27785
58.50				70.48146
59.00				71.96797
59.25				72.94513
59.30				73.19900

Table 19 β vs. θ_b for Taylor-Maccoll flow; $M_1=10.0$; weak solution

θ_b	β			
	perfect gas	imperfect gas		
		Θ_{v0}		
		5.0	1.5	0.5
0.00	90.00000	90.00000	90.00000	90.00000
2.50	89.97888	89.97888	89.98006	89.98268
5.00	89.91650	89.91651	89.92113	89.93148
7.50	89.81465	89.81468	89.82487	89.84834
10.00	89.67650	89.67655	89.69480	89.73580
12.50	89.50393	89.50401	89.53201	89.59566
15.00	89.30148	89.30158	89.34175	89.43058
17.50	89.07037	89.07051	89.12335	89.24212
20.00	88.81061	88.81079	88.87918	89.03152
22.50	88.52574	88.52596	88.60997	88.80075
25.00	88.21435	88.21461	88.31734	88.54876
27.50	87.87548	87.87579	87.99723	88.27490
30.00	87.50716	87.50752	87.65131	87.97781
32.50	87.10627	87.10668	87.27299	87.65703
35.00	86.66585	86.66632	86.86216	87.30586
37.50	86.18149	86.18202	86.40859	86.92355
40.00	85.64128	85.64188	85.90354	86.49981
42.50	85.02831	85.02899	85.33472	86.02544
45.00	84.32161	84.32239	84.68113	85.48757
47.50	83.48517	83.48605	83.90690	84.86425
50.00	82.44415	82.44516	82.96369	84.11786
52.50	81.05869	81.05986	81.73595	83.19563
55.00	78.90848	78.90987	79.93208	81.96450
56.00	77.42688	77.43123	78.82908	81.31579
56.50	76.22043	76.22561	78.09662	80.94354
56.75	75.16391	75.18293	77.64606	80.73893
57.00			77.09526	80.52325
57.50			75.00041	80.04219
58.00				79.47137
58.50				78.76104
59.00				77.77227
59.25				77.02613
59.30				76.82959

Table 20 β vs. θ_b for Taylor-Maccoll flow; $M_1=10.0$; strong solution

θ_b	C_{pb}			
	perfect gas	imperfect gas		
		Θ_{v0}		
		5.0	1.5	0.5
0.00	.0000	.0000	.0000	.0000
2.50	.0126	.0126	.0125	.0124
5.00	.0467	.0467	.0466	.0465
7.50	.0936	.0936	.0935	.0934
10.00	.1521	.1521	.1518	.1517
12.50	.2228	.2228	.2221	.2217
15.00	.3081	.3081	.3065	.3056
17.50	.4158	.4145	.4104	.4075
19.00	.5095	.5086	.4962	.4907
19.25	.5333	.5339	.5153	.5084
19.50			.5365	.5271
19.75			.5704	.5518
20.00				.5983

Table 21 C_{pb} vs. θ_b for Taylor-Maccoll flow; $M_1= 1.2$; weak solution

θ_b	C_{pb}			
	perfect gas	imperfect gas		
		Θ_{v0}		
		5.0	1.5	0.5
0.00	.5093	.5093	.5248	.5335
2.50	.5202	.5203	.5356	.5442
5.00	.5447	.5448	.5600	.5685
7.50	.5763	.5763	.5912	.5993
10.00	.6090	.6091	.6237	.6318
12.50	.6386	.6387	.6535	.6615
15.00	.6587	.6587	.6743	.6827
17.50	.6591	.6592	.6774	.6871
19.00	.6313	.6317	.6579	.6708
19.25	.6175	.6177	.6500	.6643
19.50			.6385	.6557
19.75			.6169	.6426
20.00				.6072

Table 22 C_{pb} vs. θ_b for Taylor-Maccoll flow; $M_1= 1.2$; strong solution

θ_b	C_{pb}			
	perfect gas	imperfect gas		
		Θ_{v0}		
		5.0	1.5	0.5
0.00	.0000	.0000	.0000	.0000
2.50	.0131	.0104	.0102	.0101
5.00	.0397	.0395	.0394	.0393
7.50	.0774	.0774	.0772	.0771
10.00	.1234	.1234	.1233	.1232
12.50	.1776	.1776	.1774	.1770
15.00	.2398	.2398	.2389	.2386
17.50	.3095	.3095	.3083	.3074
20.00	.3864	.3864	.3847	.3844
22.50	.4723	.4723	.4692	.4683
25.00	.5697	.5696	.5644	.5620
27.50	.6826	.6820	.6728	.6671
28.00	.7082	.7082	.6977	.6917
29.00	.7648	.7653	.7478	.7409
30.00	.8381	.8378	.8116	.7986
30.50	.9004	.9001	.8488	.8313
31.00			.9002	.8699
31.25				.8937
31.30				.8994

Table 23 C_{pb} vs. θ_b for Taylor-Maccoll flow; $M_1= 1.5$; weak solution

θ_b	C_{pb}			
	perfect gas	imperfect gas		
		Θ_{v0}		
		5.0	1.5	0.5
0.00	.9259	.9260	.9520	.9696
2.50	.9333	.9334	.9592	.9766
5.00	.9494	.9495	.9749	.9921
7.50	.9702	.9703	.9950	1.0119
10.00	.9926	.9927	1.0170	1.0334
12.50	1.0148	1.0149	1.0387	1.0548
15.00	1.0350	1.0351	1.0586	1.0744
17.50	1.0518	1.0519	1.0753	1.0909
20.00	1.0640	1.0641	1.0877	1.1034
22.50	1.0703	1.0704	1.0946	1.1106
25.00	1.0683	1.0684	1.0941	1.1109
27.50	1.0524	1.0526	1.0820	1.1007
28.00	1.0462	1.0464	1.0772	1.0967
29.00	1.0287	1.0289	1.0640	1.0856
30.00	.9956	.9958	1.0421	1.0681
30.50	.9530	.9533	1.0245	1.0551
31.00			.9929	1.0362
31.25				1.0223
31.30				1.0188

Table 24 C_{pb} vs. θ_b for Taylor-Maccoll flow; $M_1= 1.5$; strong solution

θ_b	C_{pb}			
	perfect gas	imperfect gas		
		Θ_{v0}		
		5.0	1.5	0.5
0.00	.0000	.0000	.0000	.0000
2.50	.0098	.0098	.0097	.0097
5.00	.0340	.0340	.0339	.0339
7.50	.0654	.0654	.0653	.0652
10.00	.1039	.1039	.1038	.1037
12.50	.1501	.1501	.1499	.1494
15.00	.2021	.2021	.2015	.2010
17.50	.2603	.2603	.2592	.2588
20.00	.3250	.3250	.3244	.3230
22.50	.3958	.3958	.3950	.3927
25.00	.4733	.4733	.4703	.4689
27.50	.5559	.5559	.5532	.5490
30.00	.6465	.6442	.6394	.6368
32.50	.7402	.7402	.7338	.7309
35.00	.8442	.8442	.8357	.8280
37.50	.9603	.9602	.9468	.9347
40.00	1.1102	1.1101	1.0783	1.0558
40.50	1.1599	1.1601	1.1102	1.0834
41.00			1.1483	1.1131
41.50			1.2065	1.1463
42.00				1.1865
42.10				1.1964
42.25				1.2133

Table 25 C_{pb} vs. θ_b for Taylor-Maccoll flow; $M_1= 2.0$; weak solution

θ_b	C_{pb}			
	perfect gas	imperfect gas		
		Θ_{v0}		
		5.0	1.5	0.5
0.00	1.2500	1.2501	1.2802	1.3081
2.50	1.2549	1.2550	1.2849	1.3126
5.00	1.2657	1.2658	1.2952	1.3225
7.50	1.2794	1.2794	1.3083	1.3350
10.00	1.2943	1.2944	1.3227	1.3488
12.50	1.3092	1.3093	1.3370	1.3626
15.00	1.3234	1.3235	1.3506	1.3757
17.50	1.3362	1.3363	1.3630	1.3875
20.00	1.3471	1.3472	1.3737	1.3979
22.50	1.3560	1.3560	1.3822	1.4063
25.00	1.3623	1.3624	1.3887	1.4127
27.50	1.3660	1.3661	1.3926	1.4168
30.00	1.3663	1.3664	1.3936	1.4183
32.50	1.3625	1.3626	1.3910	1.4166
35.00	1.3527	1.3528	1.3834	1.4107
37.50	1.3320	1.3321	1.3674	1.3981
40.00	1.2783	1.2787	1.3319	1.3723
40.50	1.2477	1.2479	1.3189	1.3638
41.00			1.3000	1.3532
41.50			1.2613	1.3392
42.00				1.3182
42.10				1.3122
42.25				1.3008

Table 26 C_{pb} vs. θ_b for Taylor-Maccoll flow; $M_1= 2.0$; strong solution

θ_b	C_{pb}			
	perfect gas	imperfect gas		
		Θ_{v0}		
		5.0	1.5	0.5
0.00	.0000	.0000	.0000	.0000
2.50	.0092	.0092	.0092	.0092
5.00	.0282	.0282	.0282	.0282
7.50	.0544	.0544	.0544	.0543
10.00	.0875	.0875	.0875	.0872
12.50	.1270	.1270	.1268	.1263
15.00	.1730	.1730	.1728	.1720
17.50	.2253	.2253	.2251	.2241
20.00	.2840	.2840	.2838	.2825
22.50	.3485	.3485	.3482	.3462
25.00	.4188	.4188	.4179	.4156
27.50	.4943	.4943	.4933	.4900
30.00	.5747	.5747	.5730	.5691
32.50	.6600	.6600	.6586	.6523
35.00	.7485	.7485	.7467	.7392
37.50	.8420	.8420	.8387	.8298
40.00	.9388	.9386	.9341	.9238
42.50	1.0398	1.0398	1.0335	1.0204
45.00	1.1476	1.1476	1.1369	1.1190
47.50	1.2689	1.2694	1.2516	1.2256
48.50	1.3289	1.3292	1.3002	1.2745
49.00	1.3687	1.3686	1.3317	1.2936
49.50			1.3637	1.3177
50.00			1.4055	1.3429
50.50				1.3700
51.00				1.4000
51.25				1.4171
51.50				1.4368
51.75				1.4637

Table 27 C_{pb} vs. θ_b for Taylor-Maccoll flow; $M_1 = 3.0$; weak solution

θ_b	C_{pb}			
	perfect gas	imperfect gas		
		Θ_{v0}		
		5.0	1.5	0.5
0.00	1.4815	1.4815	1.5072	1.5479
2.50	1.4848	1.4849	1.5104	1.5508
5.00	1.4920	1.4921	1.5172	1.5570
7.50	1.5012	1.5012	1.5259	1.5649
10.00	1.5112	1.5112	1.5354	1.5737
12.50	1.5212	1.5213	1.5449	1.5823
15.00	1.5309	1.5309	1.5541	1.5907
17.50	1.5398	1.5399	1.5626	1.5986
20.00	1.5477	1.5478	1.5702	1.6055
22.50	1.5546	1.5546	1.5768	1.6116
25.00	1.5603	1.5604	1.5823	1.6168
27.50	1.5648	1.5648	1.5867	1.6210
30.00	1.5680	1.5680	1.5899	1.6242
32.50	1.5697	1.5698	1.5918	1.6263
35.00	1.5699	1.5700	1.5923	1.6272
37.50	1.5682	1.5683	1.5912	1.6268
40.00	1.5641	1.5642	1.5879	1.6248
42.50	1.5564	1.5565	1.5817	1.6207
45.00	1.5426	1.5427	1.5708	1.6134
47.50	1.5148	1.5149	1.5504	1.6006
48.50	1.4919	1.4921	1.5362	1.5927
49.00	1.4711	1.4711	1.5262	1.5878
49.50			1.5124	1.5820
50.00			1.4890	1.5750
50.50				1.5661
51.00				1.5541
51.25				1.5460
51.50				1.5352
51.75				1.5173

Table 28 C_{pb} vs. θ_b for Taylor-Maccoll flow; $M_1= 3.0$; strong solution

θ_b	C_{pb}			
	perfect gas	imperfect gas		
		Θ_{v0}		
		5.0	1.5	0.5
0.00	.0000	.0000	.0000	.0000
2.50	.0057	.0057	.0057	.0057
5.00	.0186	.0186	.0186	.0186
7.50	.0389	.0389	.0389	.0389
10.00	.0668	.0668	.0668	.0668
12.50	.1017	.1017	.1017	.1016
15.00	.1442	.1442	.1442	.1440
17.50	.1930	.1930	.1930	.1927
20.00	.2488	.2488	.2488	.2481
22.50	.3106	.3106	.3106	.3099
25.00	.3783	.3783	.3783	.3770
27.50	.4509	.4509	.4509	.4498
30.00	.5283	.5283	.5284	.5265
32.50	.6101	.6101	.6102	.6074
35.00	.6952	.6952	.6955	.6918
37.50	.7837	.7837	.7834	.7790
40.00	.8740	.8740	.8740	.8679
42.50	.9673	.9673	.9669	.9593
45.00	1.0621	1.0621	1.0611	1.0523
47.50	1.1584	1.1584	1.1564	1.1460
50.00	1.2556	1.2556	1.2528	1.2391
52.50	1.3563	1.3564	1.3509	1.3333
55.00	1.4697	1.4649	1.4535	1.4287
56.00	1.5169	1.5170	1.5018	1.4685
56.50	1.5498	1.5499	1.5266	1.4886
56.75	1.5735	1.5735	1.5407	1.4992
57.00			1.5562	1.5092
57.50			1.6031	1.5306
58.00				1.5530
58.50				1.5775
59.00				1.6060
59.25				1.6236
59.30				1.6281

Table 29 C_{pb} vs. θ_b for Taylor-Maccoll flow; $M_1= 10.0$; weak solution

θ_b	C_{pb}			
	perfect gas	imperfect gas		
		Θ_{v0}		
		5.0	1.5	0.5
0.00	1.6500	1.6500	1.6667	1.7067
2.50	1.6522	1.6523	1.6688	1.7086
5.00	1.6570	1.6570	1.6733	1.7126
7.50	1.6630	1.6631	1.6791	1.7176
10.00	1.6696	1.6696	1.6854	1.7231
12.50	1.6763	1.6763	1.6917	1.7286
15.00	1.6827	1.6827	1.6978	1.7340
17.50	1.6887	1.6887	1.7035	1.7390
20.00	1.6941	1.6942	1.7087	1.7436
22.50	1.6990	1.6990	1.7134	1.7477
25.00	1.7032	1.7032	1.7174	1.7513
27.50	1.7067	1.7067	1.7208	1.7544
30.00	1.7096	1.7096	1.7236	1.7569
32.50	1.7118	1.7119	1.7258	1.7590
35.00	1.7134	1.7134	1.7273	1.7605
37.50	1.7142	1.7142	1.7282	1.7615
40.00	1.7142	1.7142	1.7284	1.7620
42.50	1.7133	1.7133	1.7277	1.7618
45.00	1.7112	1.7112	1.7259	1.7609
47.50	1.7075	1.7075	1.7228	1.7590
50.00	1.7012	1.7013	1.7175	1.7557
52.50	1.6906	1.6907	1.7088	1.7505
55.00	1.6695	1.6695	1.6923	1.7415
56.00	1.6519	1.6520	1.6804	1.7360
56.50	1.6359	1.6360	1.6717	1.7327
56.75	1.6207	1.6210	1.6661	1.7307
57.00			1.6589	1.7286
57.50			1.6289	1.7238
58.00				1.7177
58.50				1.7096
59.00				1.6974
59.25				1.6875
59.30				1.6848

Table 30 C_{pb} vs. θ_b for Taylor-Maccoll flow; $M_1= 10.0$; strong solution

M_1	$\frac{\beta_{\delta=1}}{\beta_{\delta=0}}$		
	Θ_{v0}		
	5.0	1.5	0.5
1.075	.99998	.99758	.99645
1.100	.99999	.99841	.99764
1.200	1.00000	.99907	.99858
1.300	1.00000	.99918	.99870
1.400	1.00000	.99919	.99866
1.500	1.00000	.99916	.99855
1.750	1.00000	.99906	.99812
2.000	1.00000	.99899	.99758
2.500	1.00000	.99913	.99640
3.000	1.00000	.99950	.99535
3.500	1.00000	.99979	.99463
3.750	1.00000	.99988	.99445
4.000	1.00000	.99994	.99438
4.250	1.00000	.99997	.99445
4.500	1.00000	.99999	.99465
4.750	1.00000	.99999	.99496
5.000	1.00000	1.00000	.99537
5.250	1.00000	1.00000	.99585
5.500	1.00000	1.00000	.99636
6.000	1.00000	1.00000	.99738
6.500	1.00000	1.00000	.99825
7.000	1.00000	1.00000	.99890
7.500	1.00000	1.00000	.99934
8.000	1.00000	1.00000	.99961
8.500	1.00000	1.00000	.99978
9.000	1.00000	1.00000	.99987
9.500	1.00000	1.00000	.99993
10.000	1.00000	1.00000	.99996

Table 31 β -ratio vs. M_1 for Taylor-Maccoll flow; $\theta_b=10^\circ$; weak solution

M_1	$\frac{\beta_{\delta=1}}{\beta_{\delta=0}}$		
	Θ_{v0}		
	5.0	1.5	0.5
1.075	1.00002	1.00333	1.00487
1.100	1.00002	1.00235	1.00346
1.200	1.00001	1.00134	1.00201
1.300	1.00001	1.00104	1.00159
1.400	1.00000	1.00088	1.00138
1.500	1.00000	1.00079	1.00126
1.750	1.00000	1.00064	1.00110
2.000	1.00000	1.00056	1.00102
2.500	1.00000	1.00044	1.00094
3.000	1.00000	1.00037	1.00090
3.500	1.00000	1.00032	1.00086
4.000	1.00000	1.00028	1.00083
4.500	1.00000	1.00026	1.00081
5.000	1.00000	1.00025	1.00078
5.500	1.00000	1.00024	1.00076
6.000	1.00000	1.00023	1.00074
6.500	1.00000	1.00022	1.00072
7.000	1.00000	1.00022	1.00071
7.500	1.00000	1.00022	1.00070
8.000	1.00000	1.00021	1.00069
8.500	1.00000	1.00021	1.00068
9.000	1.00000	1.00021	1.00067
9.500	1.00000	1.00021	1.00067
10.000	1.00000	1.00020	1.00066

Table 32 β -ratio vs. M_1 for Taylor-Maccoll flow; $\theta_b=10^\circ$; strong solution

M_1	$\frac{(C_{pb})_{\delta=1}}{(C_{pb})_{\delta=0}}$		
	Θ_{v_0}		
	5.0	1.5	0.5
1.075	.99996	.99418	.99148
1.100	.99998	.99650	.99482
1.200	.99999	.99828	.99737
1.300	1.00000	.99866	.99787
1.400	1.00000	.99881	.99804
1.500	1.00000	.99889	.99809
1.750	1.00000	.99899	.99802
2.000	1.00000	.99909	.99784
2.500	1.00000	.99936	.99742
3.000	1.00000	.99967	.99707
3.500	1.00000	.99987	.99687
3.750	1.00000	.99993	.99684
4.000	1.00000	.99996	.99687
4.250	1.00000	.99998	.99696
4.500	1.00000	.99999	.99711
4.750	1.00000	1.00000	.99730
5.000	1.00000	1.00000	.99754
5.250	1.00000	1.00000	.99781
5.500	1.00000	1.00000	.99809
6.000	1.00000	1.00000	.99863
6.500	1.00000	1.00000	.99909
7.000	1.00000	1.00000	.99942
7.500	1.00000	1.00000	.99965
8.000	1.00000	1.00000	.99980
8.500	1.00000	1.00000	.99988
9.000	1.00000	1.00000	.99993
9.500	1.00000	1.00000	.99996
10.000	1.00000	1.00000	.99998

Table 33 C_{pb} -ratio vs. M_1 for Taylor-Maccoll flow; $\theta_b=10^\circ$; weak solution

M_1	$\frac{(C_{pb})_{\delta=1}}{(C_{pb})_{\delta=0}}$		
	Θ_{v0}		
	5.0	1.5	0.5
1.075	1.00016	1.02341	1.03504
1.100	1.00015	1.02270	1.03429
1.200	1.00014	1.02412	1.03742
1.300	1.00012	1.02475	1.03934
1.400	1.00011	1.02481	1.04042
1.500	1.00010	1.02458	1.04108
1.750	1.00007	1.02344	1.04186
2.000	1.00006	1.02192	1.04210
2.500	1.00004	1.01873	1.04192
3.000	1.00004	1.01602	1.04133
3.500	1.00003	1.01408	1.04052
4.000	1.00003	1.01277	1.03957
4.500	1.00003	1.01189	1.03853
5.000	1.00003	1.01128	1.03748
5.500	1.00003	1.01084	1.03647
6.000	1.00003	1.01051	1.03557
6.500	1.00002	1.01026	1.03480
7.000	1.00002	1.01006	1.03415
7.500	1.00002	1.00990	1.03361
8.000	1.00002	1.00977	1.03317
8.500	1.00002	1.00966	1.03281
9.000	1.00002	1.00957	1.03250
9.500	1.00002	1.00950	1.03224
10.000	1.00002	1.00943	1.03202

Table 34 C_{pb} -ratio vs. M_1 for Taylor-Maccoll flow; $\theta_b=10^\circ$; strong solution

M_1	$\frac{(M_2)_{\delta=1}}{(M_2)_{\delta=0}}$		
	Θ_{v_0}		
	5.0	1.5	0.5
1.075	1.00001	1.00200	1.00294
1.100	1.00001	1.00150	1.00222
1.200	1.00000	1.00107	1.00164
1.300	1.00000	1.00102	1.00162
1.400	1.00000	1.00106	1.00175
1.500	1.00000	1.00113	1.00194
1.750	1.00000	1.00133	1.00264
2.000	1.00000	1.00150	1.00356
2.500	1.00000	1.00144	1.00587
3.000	1.00000	1.00095	1.00843
3.500	1.00000	1.00044	1.01076
3.750	1.00000	1.00027	1.01170
4.000	1.00000	1.00015	1.01241
4.250	1.00000	1.00008	1.01285
4.500	1.00000	1.00004	1.01299
4.750	1.00000	1.00002	1.01283
5.000	1.00000	1.00001	1.01236
5.250	1.00000	1.00000	1.01165
5.500	1.00000	1.00000	1.01073
6.000	1.00000	1.00000	1.00856
6.500	1.00000	1.00000	1.00637
7.000	1.00000	1.00000	1.00447
7.500	1.00000	1.00000	1.00302
8.000	1.00000	1.00000	1.00197
8.500	1.00000	1.00000	1.00127
9.000	1.00000	1.00000	1.00081
9.500	1.00000	1.00000	1.00051
10.000	1.00000	1.00000	1.00033

Table 35 M_2 -ratio vs. M_1 for Taylor-Maccoll flow; $\theta_b=10^\circ$; weak solution

M_1	$\frac{(M_2)_{\delta=1}}{(M_2)_{\delta=0}}$		
	Θ_{v_0}		
	5.0	1.5	0.5
1.075	.99999	.99873	.99805
1.100	1.00000	.99908	.99846
1.200	1.00001	.99873	.99738
1.300	1.00002	.99781	.99521
1.400	1.00003	.99673	.99256
1.500	1.00004	.99559	.98963
1.750	1.00006	.99296	.98177
2.000	1.00007	.99103	.97396
2.500	1.00009	.98950	.96022
3.000	1.00011	.98994	.94987
3.500	1.00011	.99090	.94275
4.000	1.00012	.99174	.93828
4.500	1.00012	.99235	.93579
5.000	1.00013	.99279	.93468
5.500	1.00013	.99311	.93442
6.000	1.00013	.99335	.93459
6.500	1.00013	.99354	.93494
7.000	1.00013	.99368	.93532
7.500	1.00013	.99380	.93567
8.000	1.00013	.99390	.93598
8.500	1.00013	.99398	.93624
9.000	1.00013	.99405	.93645
9.500	1.00013	.99410	.93664
10.000	1.00013	.99415	.93680

Table 36 M_2 -ratio vs. M_1 for Taylor-Maccoll flow; $\theta_b = 10^\circ$; strong solution

M_1	$\frac{(M_b)_{\delta=1}}{(M_b)_{\delta=0}}$		
	Θ_{v0}		
	5.0	1.5	0.5
1.075	1.00003	1.00457	1.00671
1.100	1.00003	1.00409	1.00605
1.200	1.00002	1.00378	1.00576
1.300	1.00001	1.00384	1.00605
1.400	1.00001	1.00395	1.00647
1.500	1.00001	1.00407	1.00695
1.750	1.00000	1.00425	1.00827
2.000	1.00000	1.00418	1.00967
2.500	1.00000	1.00326	1.01246
3.000	1.00000	1.00188	1.01496
3.500	1.00000	1.00081	1.01685
3.750	1.00000	1.00049	1.01746
4.000	1.00000	1.00028	1.01780
4.250	1.00000	1.00015	1.01784
4.500	1.00000	1.00008	1.01756
4.750	1.00000	1.00004	1.01695
5.000	1.00000	1.00002	1.01605
5.250	1.00000	1.00001	1.01491
5.500	1.00000	1.00000	1.01358
6.000	1.00000	1.00000	1.01068
6.500	1.00000	1.00000	1.00788
7.000	1.00000	1.00000	1.00553
7.500	1.00000	1.00000	1.00373
8.000	1.00000	1.00000	1.00245
8.500	1.00000	1.00000	1.00158
9.000	1.00000	1.00000	1.00101
9.500	1.00000	1.00000	1.00065
10.000	1.00000	1.00000	1.00041

Table 37 M_b -ratio vs. M_1 for Taylor-Maccoll flow; $\theta_b=10^\circ$; weak solution

M_1	$\frac{(M_b)_{\delta=1}}{(M_b)_{\delta=0}}$		
	Θ_{v0}		
	5.0	1.5	0.5
1.075	1.00001	1.00097	1.00127
1.100	1.00002	1.00123	1.00155
1.200	1.00003	1.00057	1.00003
1.300	1.00004	.99944	.99756
1.400	1.00004	.99818	.99469
1.500	1.00005	.99692	.99159
1.750	1.00007	.99406	.98346
2.000	1.00009	.99198	.97548
2.500	1.00011	.99026	.96155
3.000	1.00012	.99058	.95109
3.500	1.00012	.99146	.94389
4.000	1.00013	.99225	.93936
4.500	1.00013	.99282	.93683
5.000	1.00013	.99324	.93569
5.500	1.00013	.99354	.93539
6.000	1.00014	.99377	.93554
6.500	1.00014	.99395	.93587
7.000	1.00014	.99409	.93623
7.500	1.00014	.99420	.93657
8.000	1.00014	.99430	.93686
8.500	1.00014	.99437	.93711
9.000	1.00014	.99443	.93732
9.500	1.00014	.99449	.93750
10.000	1.00014	.99453	.93765

Table 38 M_b -ratio vs. M_1 for Taylor-Maccoll flow; $\theta_b=10^\circ$; strong solution